DUDLEY KNOX LIBRARY
NAVAL POSTGRADUATE SCHOOL
MONTEREY CA 93943-5101

Copyright

by

Richard Edward Thomas

1994

# A: The Progression of a Catalytic Immune Response
# B: Molecular Recognition of Anions by Silica Bound Sapphyrin

by

Richard Edward Thomas, B.A.

THESIS

Presented to the Faculty of the Graduate School

of The University of Texas at Austin

in Partial Fulfillment

of the Requirements

for the Degree of

MASTER OF ARTS IN CHEMISTRY

THE UNIVERSITY OF TEXAS AT AUSTIN

AUGUST, 1994

T424
c.1

DUDLEY KNOX LIBRARY
NAVAL POSTGRADUATE SCHOOL
MONTEREY CA 93943-5101

A: The Progression of a Catalytic Immune Response

B: Molecular Recognition of Anions by Silica Bound Sapphyrin

## Dedication

To the memory of my uncle, Robert Blinn. His devotion to duty will always serve as an inspiration. Also in loving memory of two great men, my grandfathers, Billy Thomas and John Blinn.

## Acknowledgments

Most importantly, I must thank my parents, Raymond and Carol Thomas. Their patience, understanding, and continuous encouragement has been the key to success throughout my entire life.

I wish to thank my supervising professors for their guidance and unselfish support. I am very grateful to Dr. Brent Iverson for entrusting me with the opportunity to participate in some truly groundbreaking research projects. Thanks to Dr. Jon Sessler for helping me to make the transition into the life of a scientist.

I am extremely grateful to my fellow researchers in both Dr. Sessler's and Dr. Iverson's labs. There is Kevin Shreder who patiently taught me many needed skills and always provided honest, straightforward opinions. Thanks to Vladimir Kral who provided much beneficial guidance, in addition to synthesizing the sapphyrin-modified silica gels. Finally, thanks to Mike Wallace for synthesizing the hapten and substrate used in the antibody project.

I also want to express my gratitude to the United States Navy for providing this educational opportunity through the CIVINS program.

Submitted to Committee: 11 July,1994

# ABSTRACT

**PART A: THE PROGRESSION OF A CATALYTIC IMMUNE RESPONSE**

**PART B: MOLECULAR RECOGNITION OF ANIONS BY SILICA BOUND SAPPHYRIN**

by

**RICHARD EDWARD THOMAS**

**THE UNIVERSITY OF TEXAS AT AUSTIN, 1994**

**SUPERVISORS: BRENT L. IVERSON and JONATHAN L. SESSLER**

**Part A:** This thesis describes the first detailed study of how a catalytic immune response matures over a series of immunizations. Specifically, three male New Zealand White rabbits were immunized with a 4-(carboxy)benzyl phenyl phosphate hapten conjugated to keyhole limpet hemocyanin (KLH). The three rabbits received an initial immunization with the immunogen, followed by three immunizations at three week intervals. Serum samples were obtained from each rabbit ten days following every immunization. Pure polyclonal IgG antibodies were obtained by a multiple step

isolation and purification process. The catalytic activity of each sample was demonstrated by the rate enhancement and catalytic efficiency of the hydrolysis of the corresponding carbonate substrate. The results show a remarkable similarity in the immune response maturation seen in two of the three rabbits. The third rabbit was diseased and lagged slightly behind. Through the four immunizations, the immune response continued to optimize due to an apparent increase in the affinity of the polyclonal antibodies.

This is quite significant, in that it provides the first experimental evidence that affinity maturation is important for antibody catalysis. We have thus begun to shed the first rays of light inside the black box that produces catalytic antibodies.

**Part B**: A novel sapphyrin-functionalized silica gel has been used to study the anionic binding properties of the expanded porphyrin sapphyrin. The preparation of the first generation of this type of support is discussed. The silica-bound sapphyrin displayed longer retention times under neutral, isochratic HPLC conditions, for molecules with sterically accessible oxyanions. In particular, the sapphyrin-functionalized silica gel showed a remarkable preference for arsonates and phosphates. Furthermore, mixtures of nucleotides and oligonucleotides were cleanly separated according to the number of phosphate units they possessed. Thus, not only does sapphyrin-bound silica gel provide an exquisite way

to investigate anion binding specificities of sapphyrin, it also provides a viable method to selectively separate and analyze anion types. These types of modified silica gels may be useful for solving present day environmental problems, as well as separating and analyzing phosphorylated biologically relevant molecules.

## Table of Contents

Part A: Abstract.....vii

Part B: Abstract.....viii

List of Tables..... .xv

List of Figures..... .xv

Part A: Research Objectives and Aims.....1

Part A: Background and Significance

Immune Response.....3

Antibodies.....3

The Origin of Diversity in the Immune Response.....4

Clonal Selection.....5

Heterogeneity of the Immune Response.....6

Maturation of the Immune Response.....7

Current Model for Immune Response Maturation.....9

Kinetics of the Immune Response.....9

Monoclonal vs. Polyclonal Antibodies.....10

Catalytic Antibodies.....11

Monoclonal Catalytic Antibodies.....11

Monoclonal vs. Polyclonal Catalytic Antibodies.....12

Catalytic Polyclonal Antibodies.....14

Chemical Kinetics.....22

Part A: System Design.....26

Part A: Results

Hapten Synthesis.....29

Substrate Synthesis.....29

Immunization Regimen.....32

ELISA.....32

Antibody Isolation and Prification.....33

Background Rate Determination.....34

Prebleed Serum Activity.....34

Theoretical Inhibition Plots.....35

Inhibition Studies.....37

Catalytic Assays.....42

Rate Enhancement and Catalytic Efficiency Determination.....47

Part A: Discussion.....49

Part A: Conclusions.....58

Part A: Experimental.....61

Part B: Research Objectives and Aims.....68

Part B: Background and Significance

Sapphyrin.....70

Modified Solid Supports.....72

Seperation of Biologically Relevant Molecules.....76

Environmental Concerns.....80

Chemical Weapons.....81

Sapphyrin Dimer.....81

Overall Significance.....82

## List of Tables


Table 1. Maturation of antibody affinity.....8

Table 2. Poyclonal catayitc varaiability.....18

Table 3. Effects of changing substrate and hapten affinity.....25

Table 4. Serum titers.....32

Table 5. IgG concentrations.....33

Table 6. Background rates.....34

Table 7. Prebleed serum activity.....35

Table 8. Inhibition data.....38

Table 9. Kinetic data.....45

Table 10. Catalytic parameters..... .46

Table 11. Summary of kinetic and catalytic data..... 50

Table 12. Retention times of AMP at varying pH..... 84

Table 13. Retention times of nucleotides..... 85

Table 14. Retention of $p(dA)_{2-6}$..... 85

Table 15. Retention of anions..... 86

Table 16. Retention of adenosine series..... 87

Table 17. Retention times of $p(dA)_{2-9}$..... 87

Table 18. Retention times of p(dA)-p(dC) mixes..... 88

Table 19. Column efficiency..... 88

Table 20. Stationary phase coverage..... 89

Table 21. Free energy per phosphate for p(dA) series... 89

Table 22. Free energy per phosphate for adenosie series..... 94

Table 23. Sapphyrin dimer titration with DNA..... 94

## List of Figures

Figure 1. Kinetics of the immune response.....10

Figure 2. Gallacher's carbonate substrate and phosphate hapten.....15

Figure 3. Trityl hydrolysis and phosphonium hapten.....16

Figure 4. Phosphate and phosphorothioate haptens.....19

Figure 5. Carboxylic acid hydrolysis.....21

Figure 6. Reaction coordinates for antibody catalyzed reaction.....24

Figure 7. Phosphate hapten and carbonate substrate.....27

Figure 8. Phosphate hapten synthesis scheme.....30

Figure 9. Carbonate substrate syntheis scheme.....31

Figure 10. Theoretical inhibition plot.....37

Figure 11a. Inhibition plots for Rabbit 2335.....39

Figure 11b. Inhibition plots for Rabbit 2336.....40

Figure 11c. Inhibition plots for Rabbit 2337.....41

Figure 12a. Inhibition plots for Rabbit 2335.....43

Figure 12b. Inhibition plots for Rabbit 2336.....44

Figure 12c. Inhibition plots for Rabbit 2337.....45

Figure 13. Maturation of affinities in rabbit antibodies.53

Figure 14. Maturation of affinities in guniea pig antibodies.....55

Figure 15. Sapphyrin and porphyrin.....70

Figure 16. Crystal structure of sapphyrin.with anion.....71

Figure 17. Chromatographic support for the optical resolution of amino acids.....74

Figure 18. Methyl amino-glucitol resin.....75

Figure 19. Synthesis of sapphyrin-silica gel scheme.....83

Figure 20. Chromatogram of $p(dA)_{2-9}$.....90

Figure 21. Chromatogram of the adenylate series..... 91

Figure 22. $P(dA)_{2-9}$ energetic graphs..... 92

Figure 23. Adenylate series energetic graphs..... 93

Figure 24. Synthesis of sapphyrin-dimer.....95

Figure 25 Supercoiled Assay..... 96

## A: Research Objectives and Aims

The primary objective of this project is to investigate how the catalytic activity of an elicited immune response matures over the course of an immunization regimen. Changes in catalytic parameters and apparent catalytic antibody affinity will be correlated in polyclonal antibody samples isolated after each of four immunizations. In particular, $v_{max}$, $k_m$, $k_{cat}$, catalytic efficiency, titer, rate enhancement, and catalytic fraction shall be evaluated. This work is important because it will elucidate for the first time when optimal catalytic activity is produced by the immune system. Moreover, watching catalytic activity evolve will provide insight into the fundamental processes involved.

In other words, this research will expand our understanding of how the catalytic immune response optimizes, and whether it is dependent on genetics or hapten structure. The understandings we gain will enable us to optimize the catalytic efficiency of other polyclonal systems and refine the focus of other important research in our lab. In addition, this research will provide valuable building blocks for investigating the feasibility of immunization based therapies and treatments for a wide range of conditions.

A final point worth making is that it is not obvious that the immune system should be capable of producing and/or optimizing catalytic antibodies. The immunization of animals with a hapten or

immunogen simply results in the production of hapten specific antibodies. Over the course of the immunization regimen, the affinity of these antibodies increases, resulting in tighter binding of antibody to hapten. What we have discovered through the following studies is that it is this increase in affinity for the hapten that results in increased catalysis. Thus, we now know that the immune system efficiently evolves catalytic activity, whether it wants to or not.

## A: Background and Significance

**Immune Response.** The humoral immune response in vertebrates is mounted to counter bacterial infections, extracellular phases of viral infections, and antigens (1). This process is controlled by a collection of proteins known as immunoglobulins or antibodies. The antibodies are produced by B lymphocyte cells found primarily in the bone marrow and spleens of mammals.

An antigen can be a protein, polysaccharide, lipoprotein, or nucleoprotein (2). To be an antigen, a macromolecule must possess both antigenicity and immunogenicity. Immunogenicity is the ability of a molecule to present itself to the immune system as foreign (i.e. nonself). Therefore, the low molecular weight haptens can actually bind to antibodies, but they cannot by themselves stimulate antibody production. They are attached to some type of carrier protein for immunization. Antigenicity describes the ability of the antigen to bind with specificity to an antibody.

**Antibodies.** Antibodies are unique proteins that bind selectively to their target molecule, or antigen (2). Antibodies are composed of two identical light chains and two identical heavy chains. The chains are bound together by disulfide linkages. Each chain contains an amino-terminal variable region (V), and a

carboxy-terminal constant region (C). The class of antibody is defined by the heavy chain C region (1).

Antibodies have a two-fold mission. Not only do they bind antigens, but they also carry out certain immunological effector functions. Different domains on the antibody perform these tasks. The Fc region carries out the effector functions. The antigen binding fragment (Fab) is where the binding pocket is located. The binding pocket is formed by the hypervariable regions of the heavy and light chains. It is quite remarkable to find out that the few hundred genes of the mammalian immune system are capable of producing as many as $10^{10}$ different antibody specificities.

Five major classes of immunoglobulins (Ig's) perform various functions during immune responses. The five classes are IgM, IgG, IgD, IgE, and IgA. When a foreign antigen is introduced into an animal, IgM is produced and released into the serum the first 2 to 3 days. IgG production begins 2 to 3 days after the IgM, and is released into the blood and the interstitial fluids. The IgG molecule has an average mass of 155 kD. It is the IgG that dominates in the later stages of the immune response, and this is the type of antibody we will be primarily concerned with.

**The Origin of Diversity in the Immune Response**. There has been a historic debate about exactly how the tremendous diversity seen in the immune response is created. At one extreme, is the older belief that an individual inherits all the necessary

tools to respond to all antigens. This is called the germ line theory. A newer idea is that the individual inherits some genes dealing with antibody specificity and generates diversity through somatic mutations, called the somatic recombination theory. The germ line theory argues that the germ line transmits all the genes necessary to create all specificity. This would mean that all the genes for encoding the variable regions are present in the cell. Theoretically, this could account for some $10^9$ specificities. Recent experimental evidence has suggested that this is not the whole story.

The somatic mutation theory argues that there is no evolutionary pressure for novel genetic combinations to survive, especially since responses to certain antigens have no survival value to the individual. The amount of genetic material that would need to be passed on would be far too large to be plausible. The somatic recombination theory holds that only a minimum of germ-line genes are passed on. The extremely diverse specificity actually results from somatic mutations of these genes during maturation of antibody producing cells. It is now widely held that somatic mutation is required to produce the high affinity antibodies that are predominant at the end of an immune response.

**Clonal Selection.** A widely accepted paradigm is the Clonal Selection Theory, which was originally proposed by Burnet (3-7). This theory states the antigen does not instruct the immune system

in what specificity is needed; rather it contacts an appropriate receptor. This contact then stimulates production and proliferation of clones of the most reactive cells. High affinity antibodies will bind most tightly, and if the antigen is present in a relatively small quantity, the high affinity antibodies will dominate the response. However, if there is a relatively high concentration of antigen, then low, medium, and high affinity antibodies may all be released during the immune response. After immunization, the level of antigen in the system slowly decreases, allowing only higher affinity receptors to be contacted, thus stimulating production of high affinity antibodies.

**Heterogeneity of the Immune Response.** There have been several early studies to demonstrate the heterogeneity of the affinities seen in the antibodies produced early in an immune response (8-13). The studies showed that even simple antigens initially produced a wide range of affinities in antibodies. The distribution of antibodies as determined by equilibrium dialysis and fluorescence quenching appeared to be Gaussian or Sipsian (14-16). These functions both represent very similar symmetric distributions of affinities. The term heterogeneity index is used to describe this spread of the normal distribution curve of affinities.

Eisen and Siskind were the first to demonstrate the diversity in antibody affinity. They immunized a rabbit with 2,4-

dinitrophenyl-bovine gamma-globulin (DNP-BGG). The antibodies were isolated and separated by fractional precipitation. The ten fractions of antibodies obtained showed a 10,000 fold difference in association constants (17).

**Maturation of the Immune Response.** There is an antibody class shift seen as the immune response matures. The initial immune response consists of IgM, with a rapid shift to IgG during the primary response. Later responses will be almost entirely IgG. There is also a concomitant refinement in the affinity of IgG antibodies. This results from increased production of the highest affinity antibodies (4).

A number of early researchers reported a progressive change in antibody affinity as the immune response progressed (9,18-26). Eisen and Siskind were able to show that rabbits immunized with DNP-BGG showed a marked increase in affinity of their antibodies as the immune response matured (17,27). The results are shown in Table 1. Similar results were obtained in guinea pigs immunized with the DNP-BGG antigen (28). Comparable results were also obtained with different antigens and varying haptenic determinants (18,29-31), and in one study similar results were seen with horses (32).

Steiner and Eisen were also able to show that a change in antibody structure is seen as the immune response matures (33). Using the B cells from immunized rabbits, they were able to prove antibodies produced later in the immune response had a higher

affinity than those produced early. McGuigan *et al.*, found evidence that the amino acid sequence of the anti-DNP antibodies produced early and late in the immune response differed (34). Later, Bernstein was able to compare the peptide maps of the Fab fragments of anti-DNP antibodies by fractionation (35). The maps were similar, leading him to conclude the differences seen by McGuigan were localized to the variable portion of the Fab.

| Antigen Dose (mg) | Time after Immunization (Weeks) 2 | 3 | 4 | 6 |
|---|---|---|---|---|
| 0.05 | --- | 9.88 (3) | 10.0 (9) | 11.1 (8) |
| 0.5 | 8.72 (6) | 10.3 (7) | 11.2 (7) | 12.7 (7) |
| 5.0 | 8.96 (17) | 9.70 (8) | 10.2 (5) | 11.0 (5) |
| 50.0 | 8.46 (6) | 8.06 (5) | 8.52 (5) | 9.54 (4) |

**Table 1.** Maturation of affinity in rabbits immunized with DNP-BGG. Affinity is given in kcal/mol. Affinity was measured by fluorescence quenching (27). The number in parenthesis represents the number of rabbits used in each experiment.

The maturation of the immune response may be the result of one of two processes. The first possibility is that a large percentage of antigen early in the immunization binds to the high affinity antibodies resulting in removal of high affinity antibodies from the serum. This also implies the antibodies produced earlier and later in the response are the same. The second possibility is that high affinity antibodies are produced in larger quantities as the response progresses.

**Current Model for Immune Response Maturation.** The current model for maturation of the immune response, as pertaining to antibody affinity, can be summarized as follows. The existing antibody producing cells compete for the antigen present in solution. As the amount of antigen decreases, the probability of it encountering only higher affinity receptors increase. This would result in the proliferation of higher affinity antibodies as the lower affinity receptor cells become less capable of binding antigen. The lower affinity cells would be unsuccessful in capturing antigen, and thus not be stimulated to reproduce. The lower affinity cells would eventually be killed off by the more "fit" high affinity cells.

**Kinetics of the Immune Response.** The first time an individual contacts an antigen the response seen is called the primary response (Figure 1). The second encounter is called the secondary response. It is nearly identical to the primary response except the latent period is much shorter, and the magnitude of the response is much greater.

In the primary response, there is an initial latent phase in which no antibody is detected. The subsequent production occurs at an exponential rate, and thus is termed the log phase. Next, there is a phase of constant production called the plateau phase. This is followed by a reduction in antibody production in the decline phase.

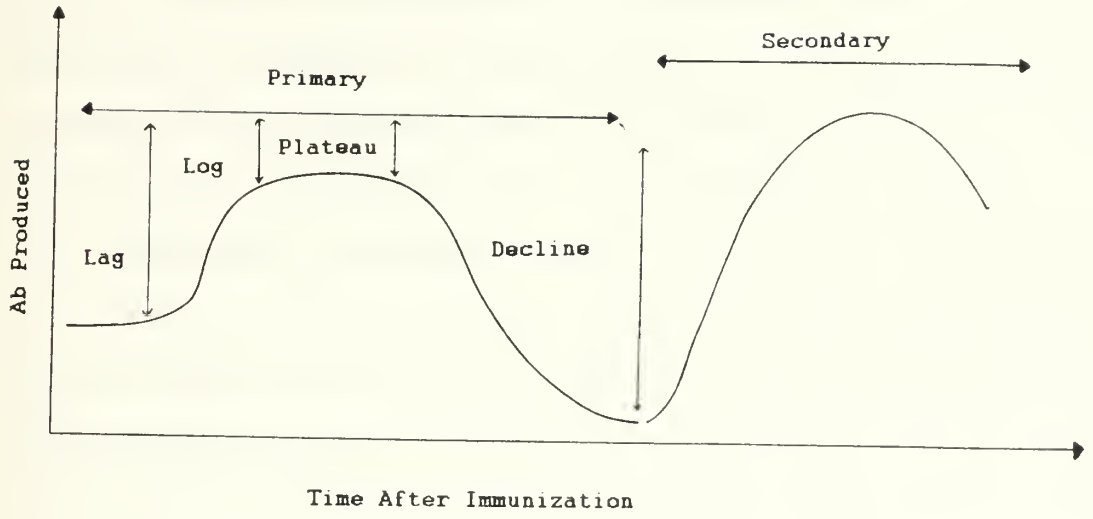


**Figure 1**. Kinetics of primary and secondary immune responses.

**Monoclonal vs. Polyclonal Antibodies**. Antibodies can be classified into two categories, monoclonal antibodies and polyclonal antibodies. Antibodies obtained directly from serum are referred to as polyclonal antibodies and represent the entire distribution of antibodies present in the serum at any one time.

Monoclonal antibodies are the most common type of catalytic antibody studied. They are obtained by immunizing an animal with the antigen (hapten) of interest. Once the proper level of immune

response is achieved, usually determined by titer, lymphocytes (B cells) are harvested from the animal. The lymphocytes are then immortalized by cell fusion with immortal myeloma cells. The clones of the resulting hybrid-myeloma, or hybridoma, are allowed to synthesize the lymphocyte's immunoglobulins. The monoclonal method produces strictly homogenous pools of antibodies. This aids in the classification and determination of the mechanism of catalysis.

**Catalytic Antibodies.** Catalytic antibodies are elicited from an animal through immunization with a chemical hapten that closely mimics a high energy intermediate or transition state for a desired reaction (36-41). The antibodies that are obtained from the animal serum presumably contain binding pockets that selectively bind the substrate. They bind in such a manner as to lower the overall transition state energy and catalyze the reaction. Thus, it is important to design transition analogs that closely mimic the transition state in every possible chemical structural feature.

**Monoclonal Catalytic Antibodies.** There have been several approaches using monoclonal antibodies to achieve catalysis. These approaches have included the use of geometry complimentarity (42-47), charge complimentarity (48,49), catalytic cofactors (50-54), medium effects (55-57), and proximity of two simultaneously bound substrates (58-63).

There are a wide variety of reactions that have been catalyzed using monoclonal antibodies. Some of the more common

reactions catalyzed include ester hydrolysis (36,56,57,64-68), amide hydrolysis (57,69), rearrangements (70), carbonate hydrolysis (37,71), lactonization (42), amide synthesis (61,62), and trans-esterification (56,57,63,72). There are also examples of antibodies catalyzing Diels-Alder reactions (58-60), Claisen rearrangements (43-45), olefin isomerization (73), a β-elimination (74), an asymmetric ketone reduction (54), phosphate hydrolysis (75), and even a photochemical cleavage reaction (76).

**Monoclonal vs. Polyclonal Catalytic Antibodies.** Using monoclonal antibodies to study antibody catalysis has allowed individual catalysts and catalytic mechanisms to be studied. However, there are several serious limitations to using the method of monoclonal antibodies. What we end up seeing is a very limited view of the overall immune response, since only a few of the antibodies actually produced by the immune response are analyzed. The randomness of this method may allow for selection of an antibody with characteristics not representative of the entire immune response. Therefore, this method fails to allow for a systematic study into hapten design and the maturation of the immune response.

Put another way, using monoclonal methods for the study of catalytic antibodies is analogous to trying to find the proverbial needle in a haystack. Nothing is known about how the immune system creates the best catalysts. If one is fortunate enough, one might

sit on the needle on the first attempt. This is not likely, so one must then enlist the help of others, buy detection equipment, fund an environmental impact study, and expend countless hours and resources trying to find a needle which may or may not exist.

In an era of shrinking research resources, one can clearly see that a method that gives us greater access to the big picture of the immune response should be further developed. This method is catalytic polyclonal antibodies. Polyclonals will allow us to uncover important trends in the overall immune response. One can then study the maturation of this response over a series of immunizations, as well as study basic trends relating hapten structure to catalytic activity. The only potential drawback in using polyclonal catalytic antibodies is that one casnnot look at the individual antibody ctructure and mechanism. This will continue to require the use of hybridomas.

An entire polyclonal study using rabbits may take as little as 4 months from design to conclusion. The cost and manpower requirements are minimal and allow for several studies, using several animals, to be conveniently carried out. On the other hand, use of monoclonal antibodies can take two to three times as long, requiring several additional time consuming processes. Thus, one is easily convinced that polyclonal catalytic antibody studies can be used to provide us with an understanding of how the entire immune system responds to varying haptenic determinants, at a substantial

saving in resources. The results obtained will provide invaluable insight into the relationship between various parameters as the immune system matures, while allowing us to design hapten systems that optimize overall antibody catalytic activity.

**Catalytic Polyclonal Antibodies.** There have been several attempts to investigate catalytic activity in polyclonal sera. There was an early attempt to produce polyclonal catalytic antibodies that could catalyze a Schiff base formation (77). There was no rate enhancement detected in the polyclonal antibodies that were produced. A later study showed polyclonal antibodies that catalyzed ester hydrolysis, but the results were not reproducible (78). Another study claimed enhancement of steroidal ester hydrolysis by immunization with the reaction product (79).

Recently, Gallacher *et al.* reported the isolation of polyclonal catalytic antibodies from the sera of sheep (80). The sheep polyclonal antibodies showed rate enhancement for the hydrolysis of the carbonate substrate **2**, shown in Figure 2, after a series of immunizations with the phosphate hapten-KLH conjugate **1**.

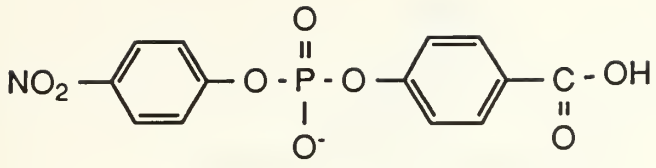

1

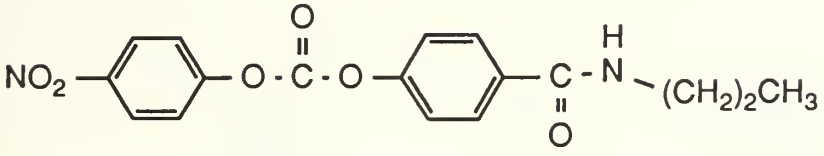

2

**Figure 2**. Carbonate substrate and phosphate hapten used in the Gallacher study.

Recent research within the Iverson group has provided substantial advancements in the field of polyclonal catalytic antibodies (81-84). The initial study, which was carried out by Stephens, involved catalyzing the hydrolysis of the triphenylmethyl ether (trityl) substrate **4**. This substrate showed a minimal background rate and allowed comparison with a previous monoclonal antibody study (48,49).

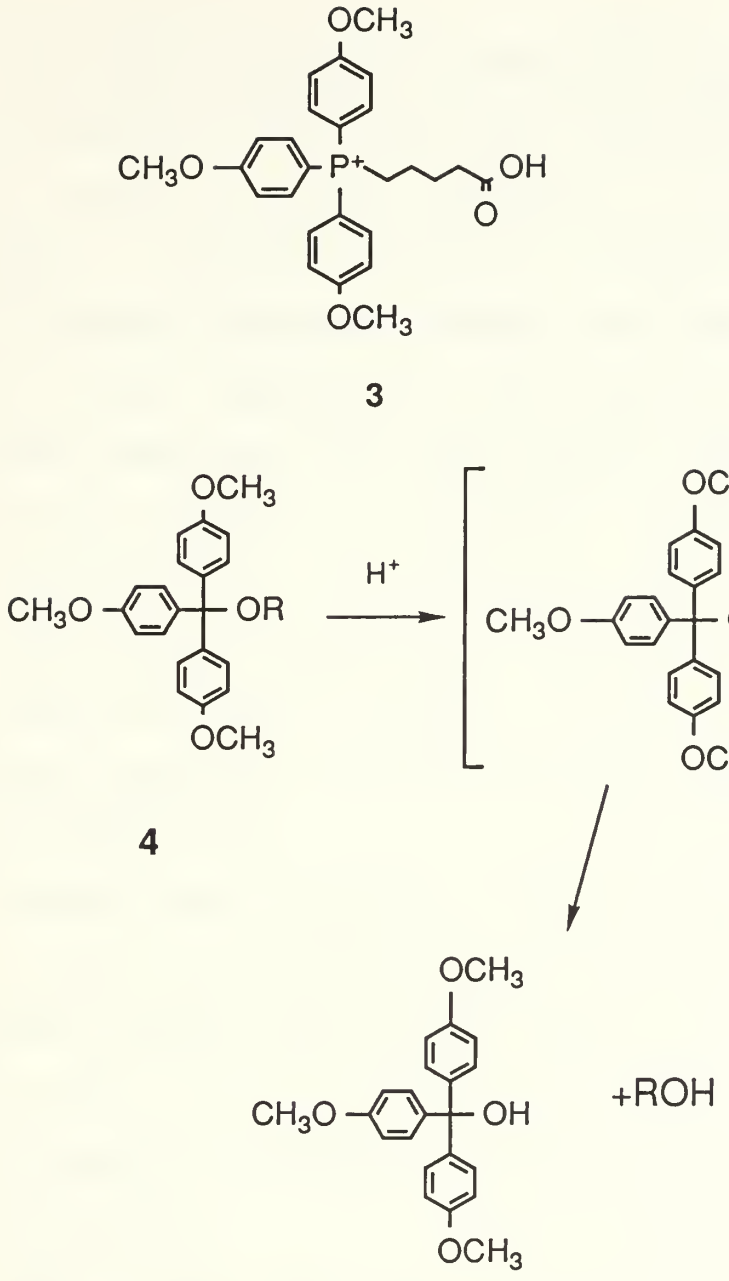


**Figure 3.** Hydrolysis of the trityl substrate, and the corresponding phosphonium hapten.

The triaryl phosphonium ion hapten **3** was used as a transition state analog for the trityl substrate **4**. The positive charge in the hapten emulates the positive charge seen in the acid catalyzed hydrolysis of the trityl substrate **4**. The polyclonal antibodies should stabilize the positive charge of the protonated substrate through charge complimentary in the antibody binding pocket, catalyzing hydrolysis of the trityl substrate. This is comparable to what was observed in the analogous monoclonal study. The monoclonal study showed a rate enhancement ($k_{cat}/k_{uncat}$) of 270.

This initial trityl hydrolysis study was a test platform of some important ideas. In addition to showing the potential of polyclonal antibodies to probe weak catalytic activity, it also showed reproducibility.

The next study consisted of five heterozygous New Zealand white rabbits being immunized five times with the hapten **3**. Polyclonal antibodies were purified from the sera collected prior to and after a series of immunizations. There was no catalytic activity present in the serum, or "prebleed," obtained prior to the first immunization.

After the last immunization, polyclonal IgG antibodies were isolated and studied in depth for catalytic activity by Stephens and myself. Catalysis studies of the polyclonal antibodies from the five rabbits showed results consistent with Michelis-Menten kinetics. The lack of significant variability in the kinetic

parameters analyzed was remarkable (see Table 2), considering that the immune system presumably chooses antibodies based on binding to hapten, and there is no selective pressure on catalytic activity.

| **Rabbit Number** | App $k_m$ ($mM^{-1}$) | App $V_{max}$ (mM/min) | App kcat ($min^{-1}$) | App kcat/ $k_{uncat}$ |
|---|---|---|---|---|
| 1 | 37 | .19 | .03 | 190 |
| 2 | 5 | .19 | .06 | 380 |
| 3 | 70 | .05 | .03 | 190 |
| 4 | 31 | .28 | .02 | 125 |
| 5 | 93 | .19 | .02 | 125 |

**Table 2.** Polyclonal catalytic variability in 5 rabbits immunized with the same hapten.

The phosphonium hapten **3** was also used as an antigen for five mice (83). Polyclonal IgG antibodies were isolated from the combined sera. Analysis of the polyclonal antibodies showed a catalytic activity with an apparent $k_{cat}$ of 0.02/min. This compares favorably with the average $k_{cat}$ of 0.03/min seen in the 5 rabbits.

It is quite interesting to compare the rate enhancements between the monoclonal and polyclonal antibodies obtained to the phosphonium hapten. The murine monoclonal antibody 37C4 showed a rate enhancement of 270 for the hydrolysis of the trityl substrate, while the polyclonal antibodies isolated from the animals immunized with the same hapten showed an apparent rate enhancement of 125 to 380. This result indicates that the same qualitative answer was generated using polyclonal antibodies at a substantial reduction in the cost of resources.

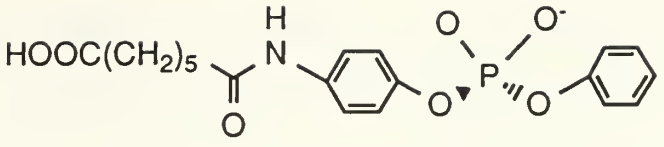


Phosphate

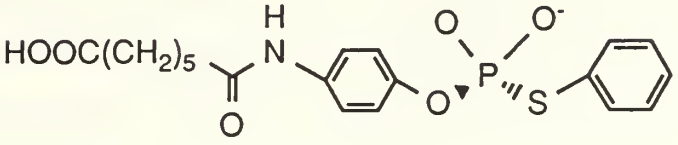


Phosphorothioate

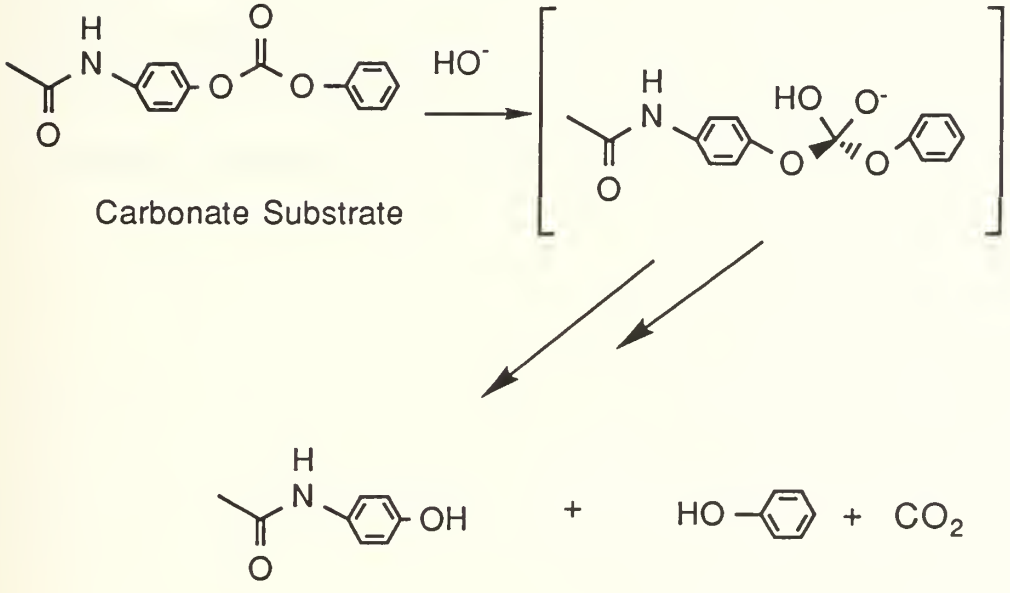


Carbonate Substrate

**Figure 4.** Phosphate and phosphorothioate hapten structures used to produce polyclonal antibodies capable of catalyzing ester and thioester hydrolysis.

Another study, by Wilmore of the Iverson group, showed catalysis of carbonate esters was possible (82). The catalytic activity was obtained using both a phosphate and phosphorothioate hapten (Figure 4). The mechanism of carboxylic acid derivative hydrolysis is shown in Figure 5 (85). The phosphate hapten showed a rate enhancement of 1800, as compared to 680 for the phosphorothioate hapten. This is in line with the rate enhancements of 800 to 10,000 for carbonate ester hydrolysis by various monoclonal antibodies (37,41,71). Once again, a polyclonal antibody study was able to show the same basic results in the catalysis of carbonate ester hydrolysis as monoclonal antibodies. The study also proved that the phosphate hapten was a better mimic of the tetrahedral intermediate, compared to the phosphorothioate.

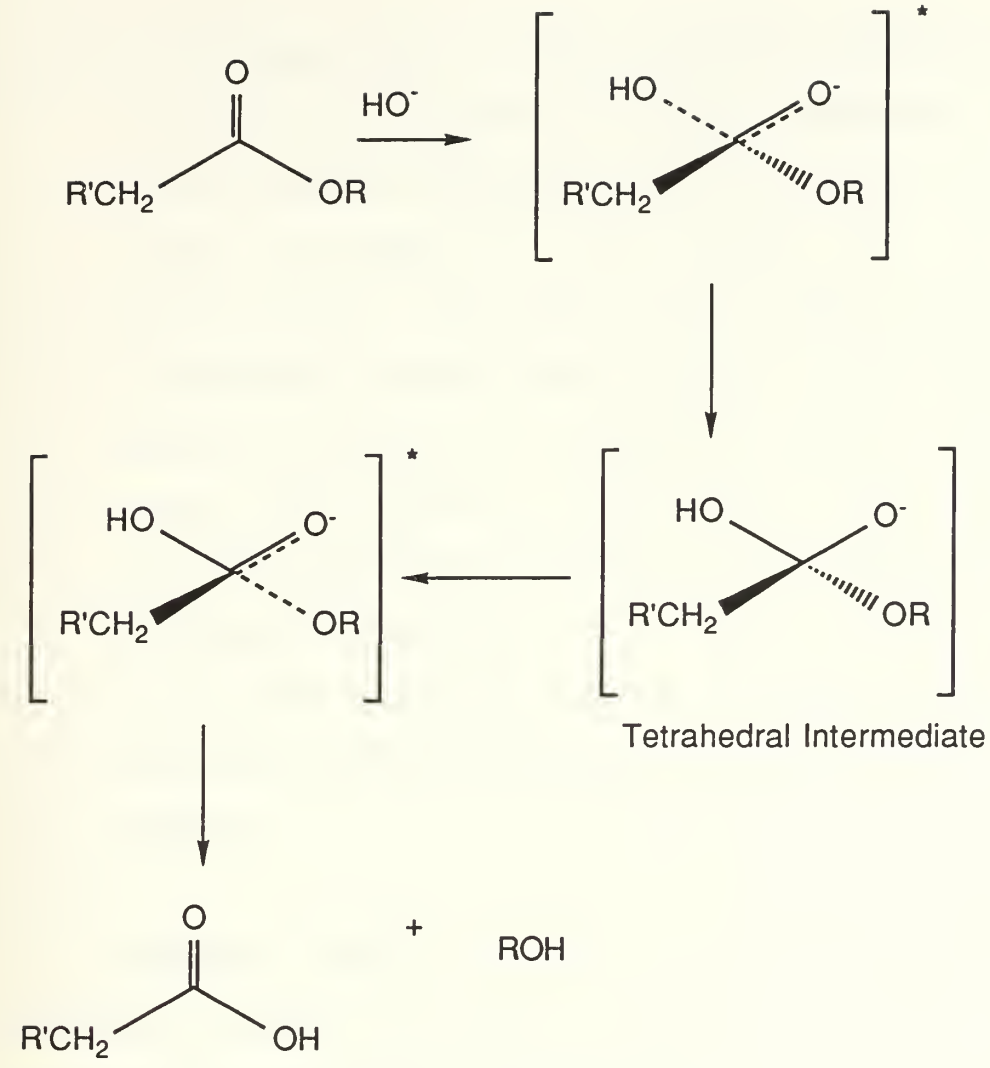


**Figure 5.** Carboxylic acid derivative hydrolysis.

To briefly summarize the significant findings with catalytic polyclonal antibodies:

1. The polyclonal catalytic antibodies isolataed from animals of the same species are shown to possess similar catalytic activity when immunized with the same hapten.

2. The results shown to date by polyclonal antibody studies provide the same conclusions as analogous monoclonal studies. It should again be emphasized that the polyclonal studies provide the results in a much quicker and much less demanding manner, while saving precious research resources.

3. Monoclonal studies focus primarily on the mechanistic aspects and selectivity of antibody catalysis. Polyclonal studies can provide us with general and systematic conclusions concerning how differences in hapten structure affect catalytic activity.

4. The most significant point to be made is catalytic polyclonal antibodies represent a composite of the entire response.

**Chemical Kinetics**. Central to this project is the assumption that over the course of the immunization regimen the affinity of the polyclonal antibodies for the hapten will increase. As already presented, this has been established through numerous earlier immunological studies.

To better understand how polyclonal catalytic antibodies are able to catalyze reactions, a brief review of chemical kinetics is in order. The fundamentals for this discussion result from the Transition State Theory first proposed by Eyring in the 1930's (1).

If one considers the basic substrate (S) reaction catalyzed by the antibody (Ab) to be:

$$Ab + S \underset{k_{-1}}{\overset{k_1}{\leftrightarrow}} Ab\text{-}S \xrightarrow{k_2} Ab + P$$

In this case, there is actually a more complex situation that involves two transition states and a tetrahedral intermediate. It will be assumed the antibody-tetrahedral intermediate activated complex lies at an energy saddle point on the reaction coordinate (Figure 6). The energy of activation is often referred to as $\Delta G^{\ddagger}$, or the Energy of Activation. Proceeding from one point in the immunization regimen to the next, the energy barrier will undergo changes as the antibody affinities change. The change in affinity for the substrate will result in a change in the energy of the antibody-substrate complex, or $\Delta G_{Ab\text{-}S}$. A change in affinity for the tetrahedral intermediate will result in a change in energy of the tetrahedral intermediate-antibody complex, or $\Delta G_{Ab\text{-}TI}$.

Catalytic antibodies are thought to catalyze reactions by increasing the stabilization of the transition state over the initial or ground state of substrate. It is important to remember that we immunize with a phosphate hapten, which mimics the charge and structure of the tetrahedral intermediate more closely than the same parameters of the substrate.

The rate enhancement realized by the reaction is directly correlated to the ratio of the stabilization of the transition

state, $\Delta\Delta G_{AB-TI}$, to the stabilization of the substrate, $\Delta\Delta G_{AB-S}$. We assume that for antibodies $k_{-1} >> k_2$, therefore:

$$k_m = (k_2 + k_{-1})/ k_1 == K_s + (k_{-2}/k_1) == K_s$$

Thus, $\Delta k_m$ is an accurate representation of $\Delta G_{Ab-S}$.

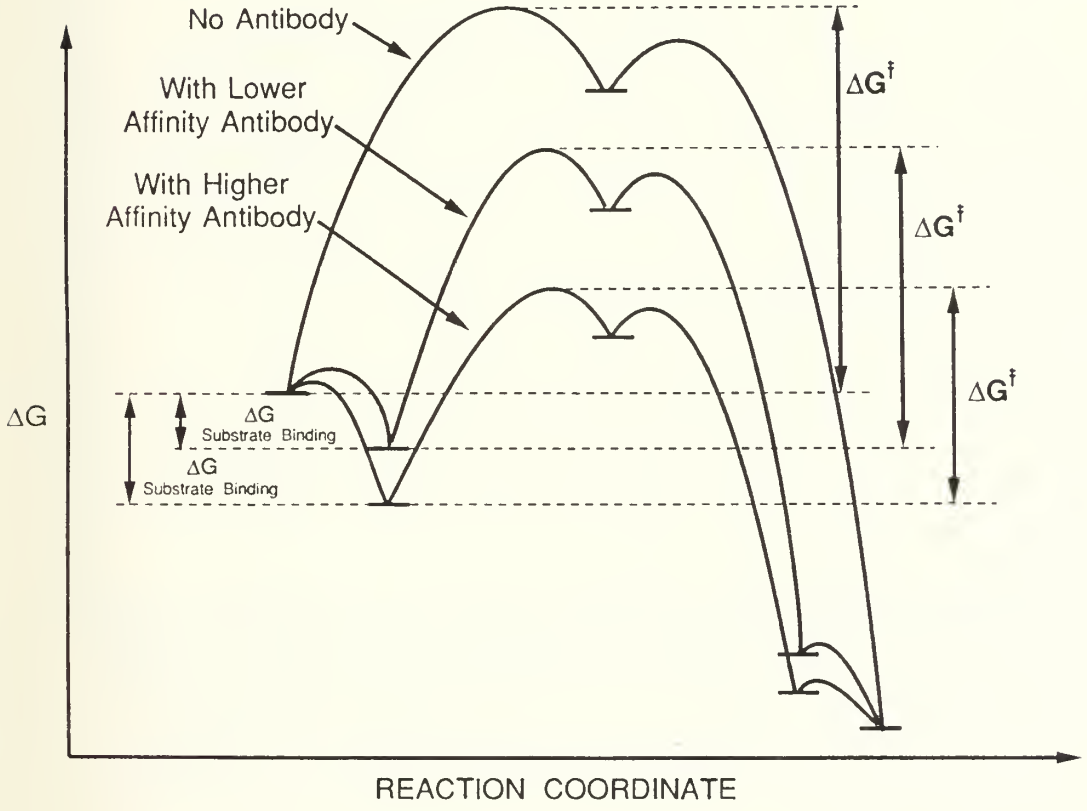


**Figure 6.** Reaction coordinates for a catalyzed reaction.

Table 3 presents an analysis of possible scenarios that occur upon immunization. The bottom line of this thought experiment is that in order to see an increase in catalytic activity we must see an increase in the affinity of antibodies for the tetrahedral intermediate. This is shown in cases 4, 6, 8, and 10 where $\Delta E_{Ab-TI}$ goes down, and catalytic activity rises.

| CASE | $\Delta G_{Ab-S}$ | $\Delta G_{Ab-TI}$ | $\Delta k_m$ | $\Delta k_{cat}$ | $\Delta$CatEff |
|---|---|---|---|---|---|
| 1 | + | + | + | 0 | - |
| 2 | + | 0 | + | + | 0 |
| 3 | 0 | + | 0 | - | - |
| 4 | + | - | + | + + | + |
| 5 | - | + | - | - - | - |
| 6 | - | - | - | 0 | + |
| 7 | - | 0 | - | - | 0 |
| 8 | 0 | - | 0 | + | + |
| 9 | 0 | 0 | 0 | 0 | 0 |
| 10 | - | - - | - | + | + + |

**Table 3**. Effects of changing antibody affinities for substrate and tetrahedral intermediate. + = increase, - = decrease, and 0 = no change.

## A: System Design

The ultimate long range goal of our lab is to be able to investigate systematically the effect that hapten structures have on the efficiency of the catalytic polyclonal antibodies produced. In order to accomplish this, one needs to first understand how the entire immune system responds and matures when challenged with a simple hapten-protein conjugate. As stated before, the polyclonal sample, unlike monoclonal samples, will be representative of the entire immune response.

The technical advantages of catalytic polyclonal antibodies are also worth repeating. They require less time from design to conclusions, cost less, are less manpower intensive, and are technically easier. Recent studies in our labs have shown us that there is little variability between different animals of the same species.

The reaction chosen to be catalyzed was a carbonate hydrolysis (Figure 7). These types of reactions are well understood mechanistically and described in the introduction. The phosphate hapten **5** was chosen as the hapten for our studies. It should most closely mimic the tetrahedral intermediate involved with hydrolysis

of substrate **6**. Gallacher *et al.* (86,92,93) previously obtained catalytic antibodies for animals immunized with a phosphate hapten.

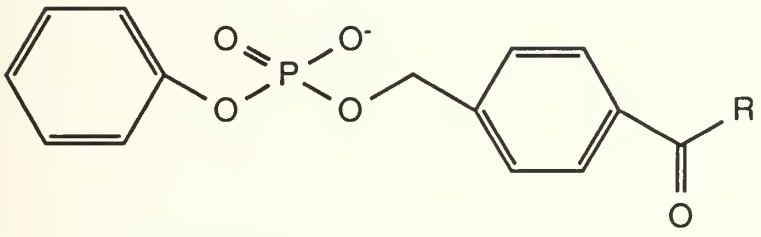


Phosphate Hapten **5**

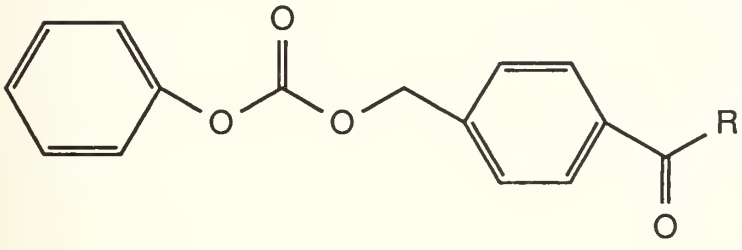


Carbonate Substrate **6**

**Figure 7**. Phosphate hapten **5** and carbonate substrate **6**.

The substrate used was chosen for several reasons. It possesses aromatic rings, which are necessary for UV detection and also provide antigenicity (2). The carbonate substrate **6** used in his study is also the first in a series of substrates that will be

used to probe the effect that slight variations in size and shape have on the catalytic antibodies produced.

## A: Results

**Hapten Synthesis**. The phosphate hapten was synthesized by Wallace in our group according to Figure 8. The first step consists of converting phosphorous trichloride to the 2-(trimethylsilyl)ethyl dichlorophosphite, by slow addition of 2-(trimethylsilyl) ethanol. After work up, the clear residue was then distilled and the fraction that boiled at 38-40$^{o}$C collected. The resulting dichlorophosphite was then reacted with diisopropylethylamine. Phenol was added, and after work up the phosphite is converted to the phosphate by using hydrogen peroxide. The final step was to deprotect the phosphate and the carboxylic acid.

The phosphate hapten was coupled to the carrier protein keyhole limpet hemocyanin (KLH) and bovine serum albumin (BSA). The KLH-hapten conjugates were used in animal immunizations, while the BSA-hapten conjugate was used in the preparation of ELISA plates.

**Substrate Synthesis**. The carbonate substrate was synthesized according to Figure 9. The first step involved coupling the pentaflourophenyl ester with butylamine. After work up the resultant benzamide was coupled with phenyl chloroformate to yield the desired carbonate.

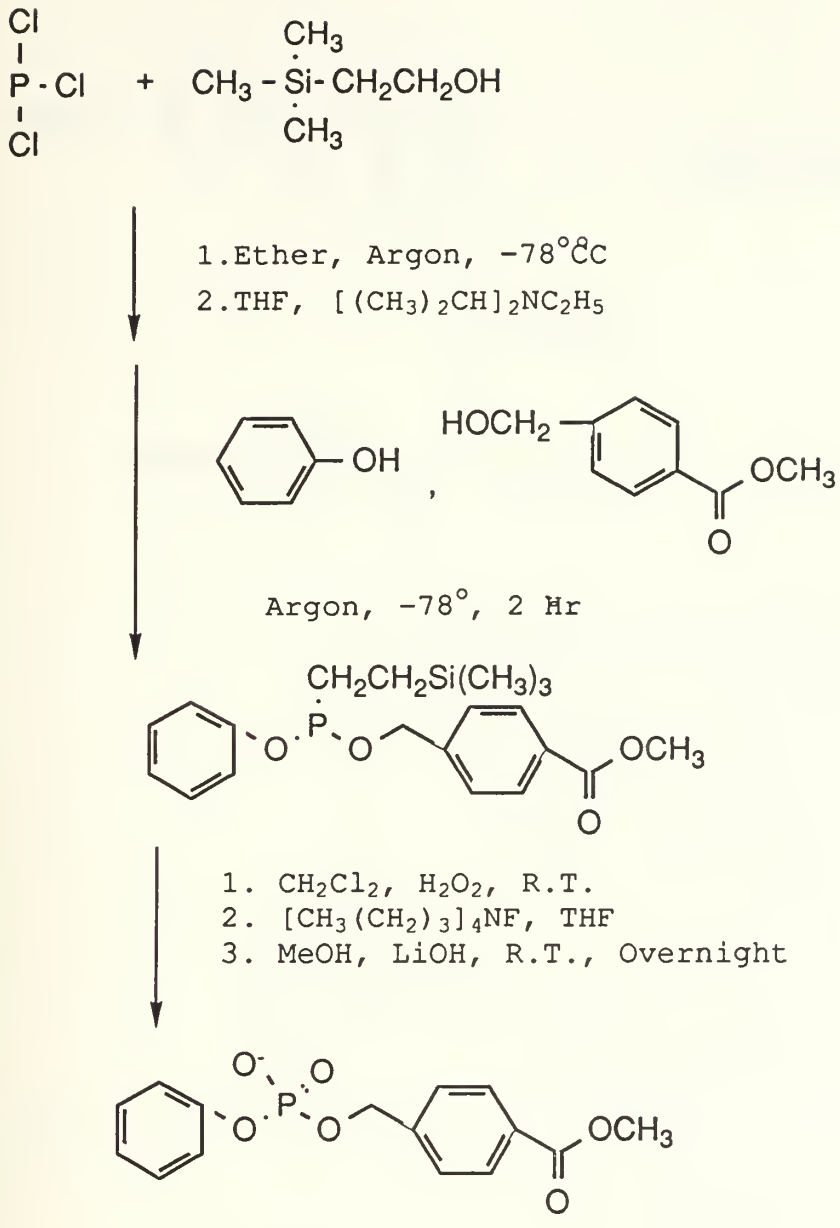


5

**Figure 8**. Synthesis of the phosphate hapten **5**.

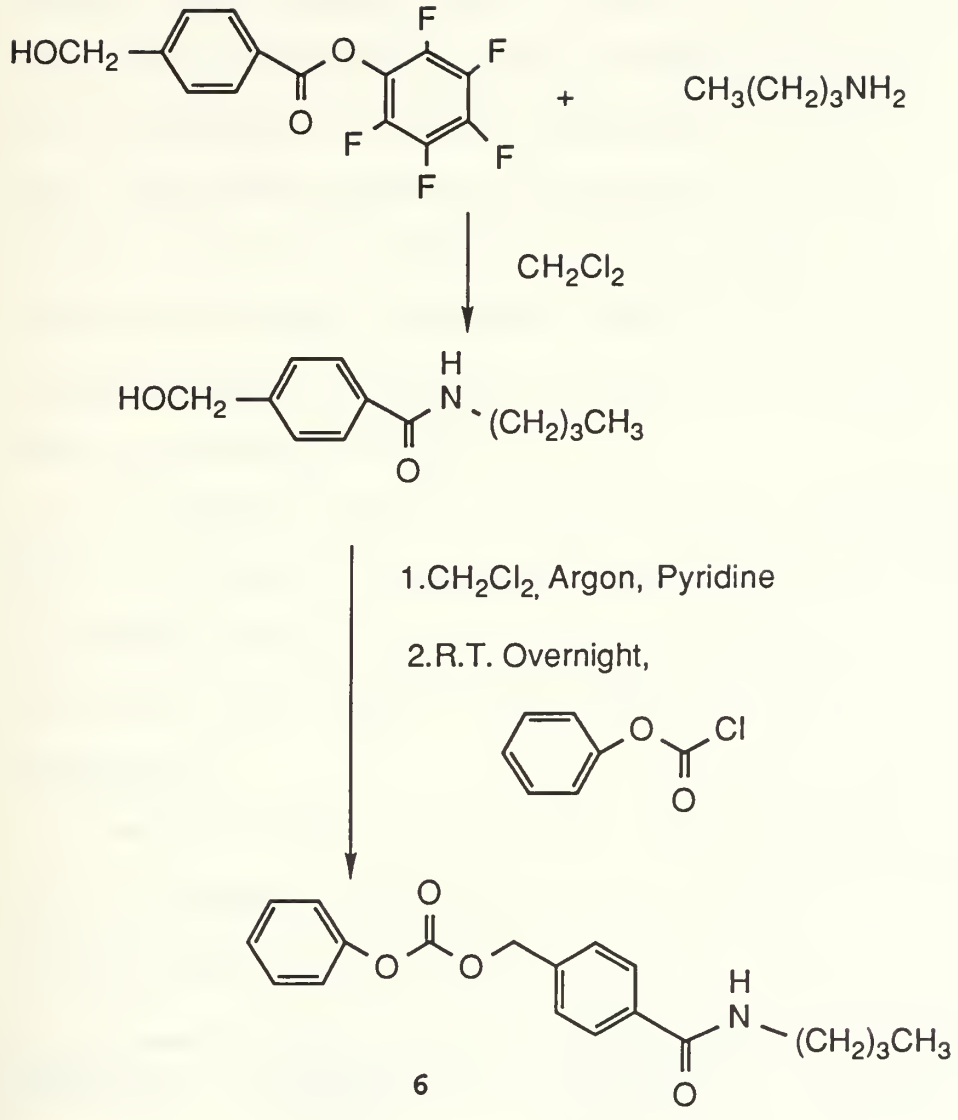


**Figure 9.** Synthesis of the carbonate substrate **6**.

**Immunization Regimen.** Serum samples from three male New Zealand white rabbits were obtained prior to the first immunization. These samples would be used to show lack of activity in the serum prior to initial immunization. At this point it was noted that Rabbit 2335 was experiencing an illness or eating disorder. Diet was adjusted, although Rabbit 2335 remained considerably thinner than rabbits 2336 and 2337. A post-mortem examination will be performed on Rabbit 2335 to determine the exact cause of this health condition.

The initial injection employed Freund's complete adjuvant with our antigen. Subsequent injections employed Freund's incomplete adjuvant. There were four injections at 21 day intervals. Serum samples were obtained 10 days after each immunization.

**Enzyme Linked Immunosorbant Assay (ELISA).** ELISA was used to determine qualitatively the amount of hapten specific antibody present in each whole serum sample.

| BLEED # | Rabbit 2335 | Rabbit 2336 | Rabbit 2337 |
|---|---|---|---|
| PREBLEED | <1/200 | <1/200 | <1/200 |
| 1 | <1/200 | 1/1,200 | 1/1,536 |
| 2 | 1/4,216 | 1/11,212 | 1/27,136 |
| 3 | 1/28,800 | 1/32,000 | 1/51,200 |
| 4 | 1/9,600 | 1/30,720 | 1/22,016 |

**Table 4.** Titers of serum samples. Each number represents the average of two ELISA's, of which each titer was read at 5 and 15 minutes.

The titer of serum obtained prior to immunization was <1/200, indicating the absence of hapten specific antibodies. We see in each case the titer of the animal increases through bleed 3, and then decreases.

**Antibody Isolation and Purification.** IgG antibodies were isolated from each of the five serum samples taken from the three rabbits. The isolation consisted of a caprylic acid precipitation, followed by an ammonium sulfate precipitation. Each sample was then purified by fast protein liquid chromatography using a Gamma Bind Protein G column. The Protein G column specifically binds IgG, which can then be eluted off be switching to a low pH buffer.

The samples were all concentrated by ultrafiltration to volumes of 0.5 to 1.5 ml. The final protein concentrations are shown in Table 5.

| SERUM SAMPLE | Rabbit 2335 mg/ml (μM) | Rabbit 2336 mg/ml (μM) | Rabbit 2337 mg/ml (μM) |
|---|---|---|---|
| PREBLEED | 6.7 (43) | 3.4 (22) | 19.3 (19) |
| 1 | 18.2 (117) | 15.2 (101) | 12.6 (81) |
| 2 | 6.6 (43) | 10.3 (66) | 6.7 (43) |
| | | 12.9 (83)* | 14.2 (91.6)* |
| 3 | 30.1 (194) | 11.2 (72) | 9.7 (63) |
| 4 | 29.9 (192) | 12.7 (82) | 18.7 (121) |
| | | | 9.0 (58)** |

**Table 5.** IgG concentrations. *Indicates a second isolation and purification were performed from original serum. **Indicates serum sample was repurified by protein G.

**Background Rate Determination.** It was important to determine the rate of the carbonate hydrolysis in the absence of catalytic antibodies. The background rate was determined by allowing a 150 μM solution of the carbonate substrate in Tris buffer at 25°C for 2 days. Background rate was also determined in the presence of the prebleed sera at antibody concentrations (16-19 μM) used for catalytic assays. The reactions were analyzed by HPLC, monitoring at 235 nm for product and substrate. Results are given in table 6.

| Sample Conditions | $k_{uncat}$ (M/min) |
|---|---|
| Buffer | $6.5 \times 10^{-5}$ ($\pm 0.28 \times 10^{-5}$) |
| With 0.1 mg/mL prebleed sera | $11.0 \times 10^{-5}$ ($\pm 2.4 \times 10^{-5}$) |
| With 0.5 mg/mL prebleed sera | $7.2 \times 10^{-5}$ ($\pm 1.5 \times 10^{-5}$) |
| With 1.0 mg/mL prebleed sera | $6.8 \times 10^{-5}$ ($\pm 1.5 \times 10^{-5}$) |
| Average in presence of prebleed sera | $8.4 \times 10^{-5}$ ($\pm 2.3 \times 10^{-5}$) |

**Table 6.** Background rates.

**Prebleed Serum Activity.** To verify the lack of catalytic activity present prior to immunization, catalytic assays using prebleed serum were conducted. The reactions consisted of 150 μM substrate and 16-19 μM serum, a second set included 16-19 μM inhibitor. The reaction was then analyzed by HPLC, monitoring at 235 nm for the precense of product and substrate. The results are shown in Table 7. There was no rate enhancement or catalytic activity seen in the prebleed serum.

| Sample | $v_{max}$ (M/min) |
|---|---|
| 2335 | $1.5 \times 10^{-8}$ |
| 2335 with/inhibitor | $1.9 \times 10^{-8}$ |
| 2336 | $4.5 \times 10^{-8}$ |
| 2336 with/inhibitor | $4.1 \times 10^{-8}$ |
| 2337 | $4.5 \times 10^{-8}$ |
| 2337 with/inhibitor | $3.4 \times 10^{-8}$ |

**Table 7.** Prebleed activity.

**Theoretical Inhibition Plots.** It was desired to prove the shapes of the inhibition plots we would obtain are similar to those predicted by the kinetics equations. Using *Mathematica* Version 2.2, it is possible to solve a series of kinetics equations and derive a theoretical inhibition plot for a polyclonal sample.

The competing reactions to be concerned with are the antibody binding with the substrate and going to product, and the antibody reversibly binding with hapten. These can be represented by the following equations (1,2):

$$S + Ab \underset{k_{-1}}{\overset{k_1}{\leftrightarrow}} AbS \xrightarrow{k_2} Ab + P$$

$$Ab + H \xrightarrow{k_H} AbH$$

From these two equations we derive a series of five equations. The first four come directly from the two reaction equations.

$$(1) \qquad k_H = \{[Ab]_F \times [H]_F\} / [AbH]$$

$$(2) \qquad [S]_T = [S]_F + [AbS]$$

(3) $$[H]_T = [H]_F + [AbH]$$

(4) $$[Ab]_T = [Ab]_f + [AbS] + [AbH]$$

The fifth equation deals with the Michelis constant, $k_M$.

$$k_M = (k_{-1} + k_2)/ k_1$$

It is assumed for catalytic antibodies that $k_{-1} >> k_2$ (1,2), therefore:

$$k_M = k_{-1}/ k_1$$

And the fifth equation follows:

(5) $$k_M = \{[Ab]_F \times [S]_F\}/ [AbS]$$

The five equations were used in the *Mathematica* program to solve for [AbS]. To further simplify this solution, values were substituted in based on known parameters from the variability study done in our labs (84). The values used were a substrate concentration of 50 μM, a $k_m$ of 50 μM, and a total antibody concentration of 6 μM. The *Mathematica* program is used to solve the five equations and yields:

$$(-2500 + 50 \times [AbS]) \times [H]_T = -15{,}000 + (5{,}300 \times [AbS]) - (50 [AbS]^2) + (5{,}600 \times k_H) - \{(15{,}000 \times k_H)/[AbS]\} - (156 \times [AbS] \times k_H\} + ([AbS]^2 \times k_H)$$

Next, values of hapten concentration, ($[H_T]$), were inserted in from 0 to 40 μM, for each value of $K_H$ plugged in. The values substituted

for $K_H$ were 100, 10, 0.99, 0.1, 0.01, 0.001, 0.0001, 0.00001, and 0.000001. The results were then plotted and compared to actual inhibition plots. The theoretical inhibition plot is shown in Figure 10. When comparing the theoretical plots to the actual plots, we can see similarity to the shape of the actual plot, and our apparent $K_H$ ($K_i$) is $\leq 1 \times 10^{-7}$ M.

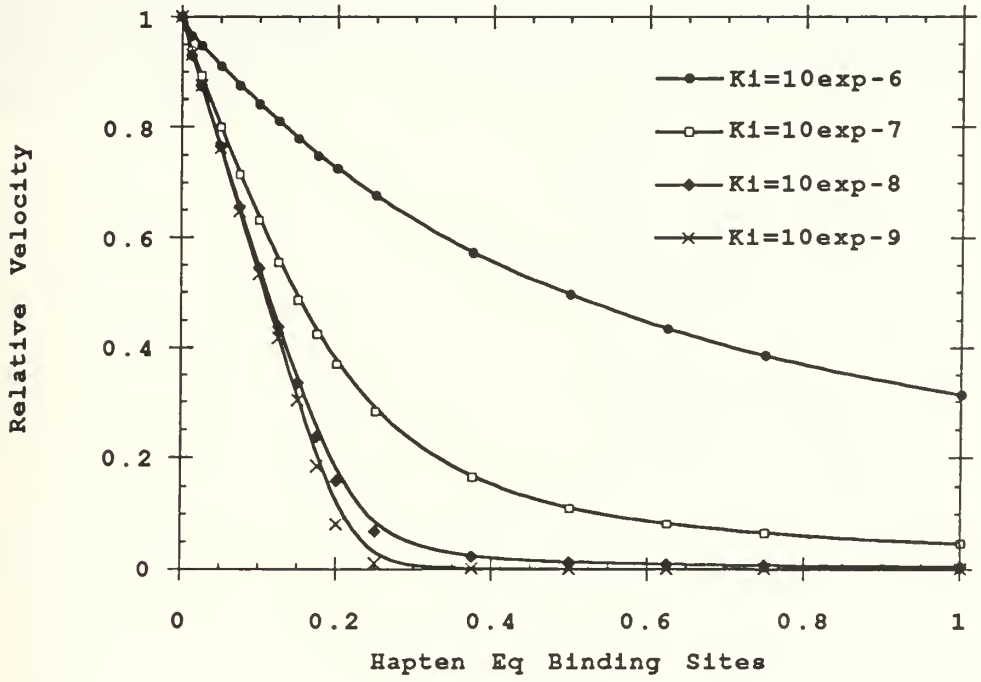


**Figure 10.** Theoretical Inhibition Plot.

**Inhibition Studies.** The hapten used for immunization was shown to be an effective inhibitor of the polyclonal antibodies

isolated. The samples that showed catalytic activity were inhibited with the hapten to determine what percentage of the isolated antibody binding sites are active. The results are shown in Table 8. The percentage of active binding sites appears to decrease slightly over the course of the immunizations. The individual inhibition plots are shown in Figure 11.

| | Rabbit 2335 | RABBIT 2336 | RABBIT 2337 |
|---|---|---|---|
| BLEED 2 | N/A | 2.0% | 8.0% |
| BLEED 3 | 3.0% | 7.0% | 8.0% |
| BLEED 4 | 2.5% | 4.0% | 6.0% |

**Table 8.** Inhibition data (each point $\pm$1%).

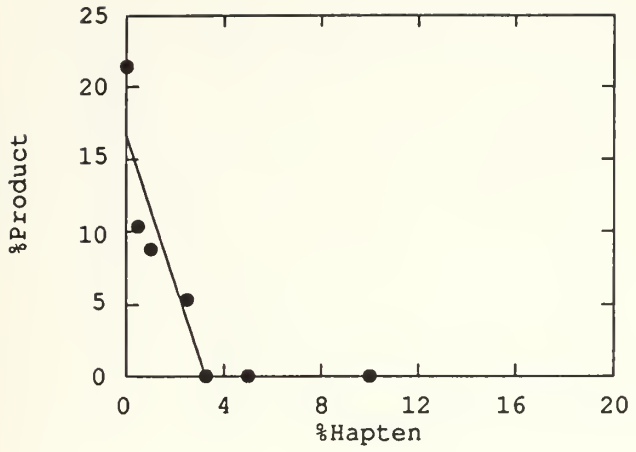


Bleed 3

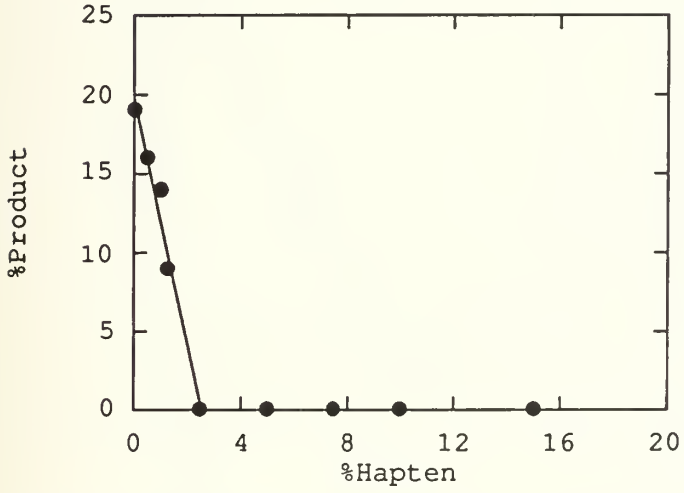


Bleed 4

**Figure 11a.** Inhibition Plots for Rabbit 2335.

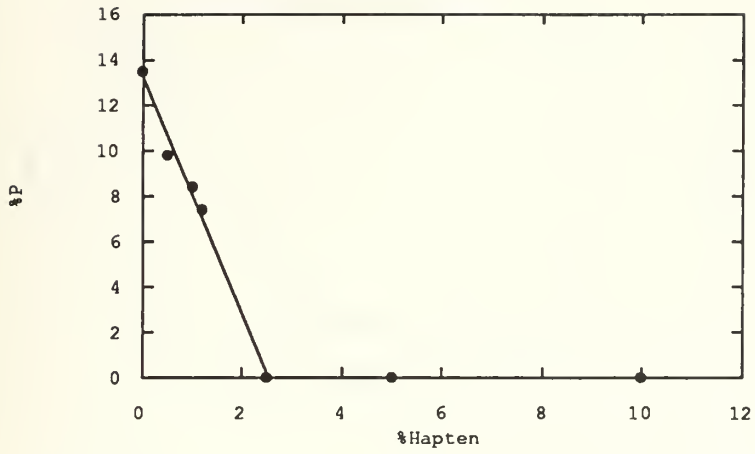


Bleed 2

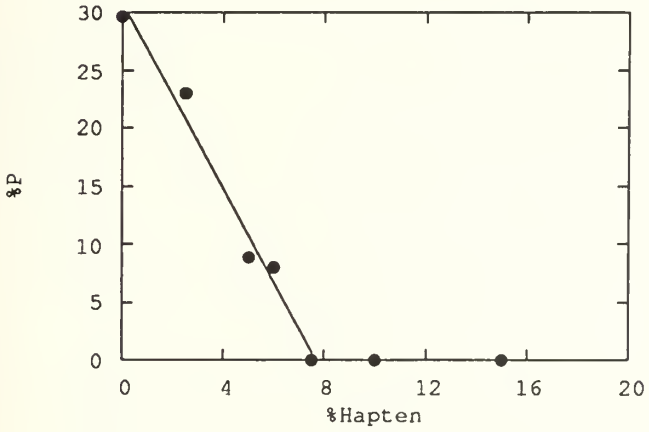


Bleed 3

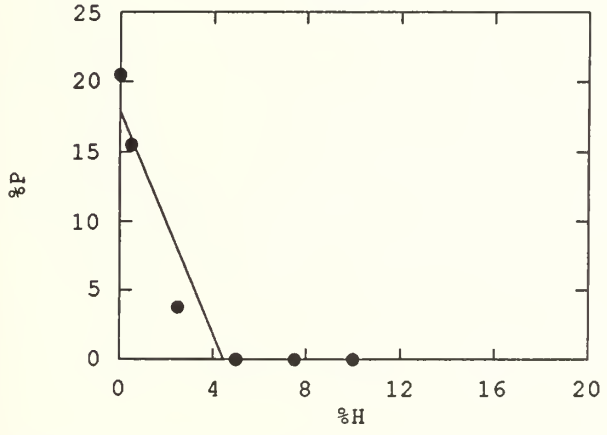


Bleed 4

**Figure 11b.** Inhibition Plots for Rabbit 2336.

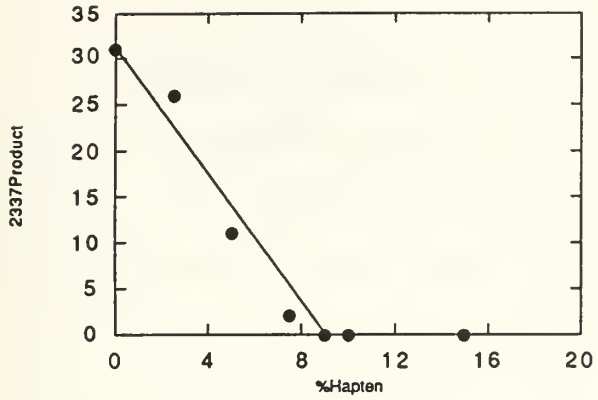


Bleed 2

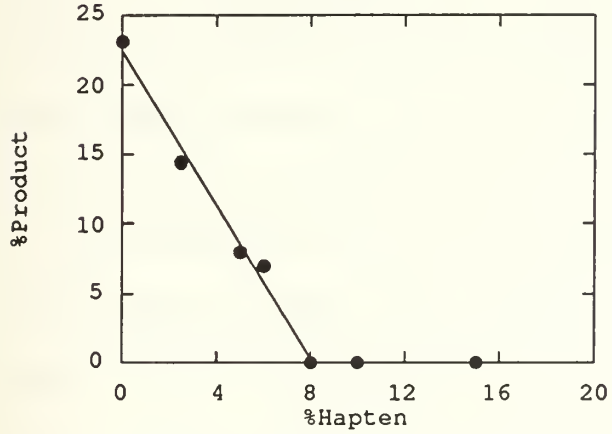


Bleed 3

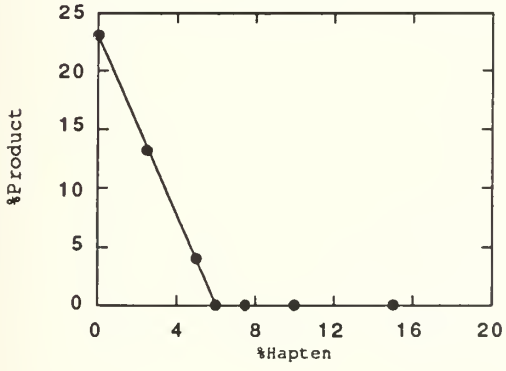


Bleed 4

**Figure 11c.** Inhibition Plots for Rabbit 2337.

**Catalytic Assays**. The samples obtained which showed evidence of catalytic activity were subjected to Lineweaver-Burk analysis. The antibody concentration was held at a constant concentration that was predetermined based on an initial check of activity. The reaction time and concentration were varied to achieve a conversion to about 20% product. Each data point was repeated in triplicate, and the inverses of the average velocities were plotted versus the inverse substrate concentration. These plots yielded values for $k_m$ and $v_{max}$. The plots are shown in Figure 12. The standard deviation was determined by plotting the three sets of data for each point separately. The values obtained for $k_m$, $v_{max}$, and standard deviations are shown in Table 9.

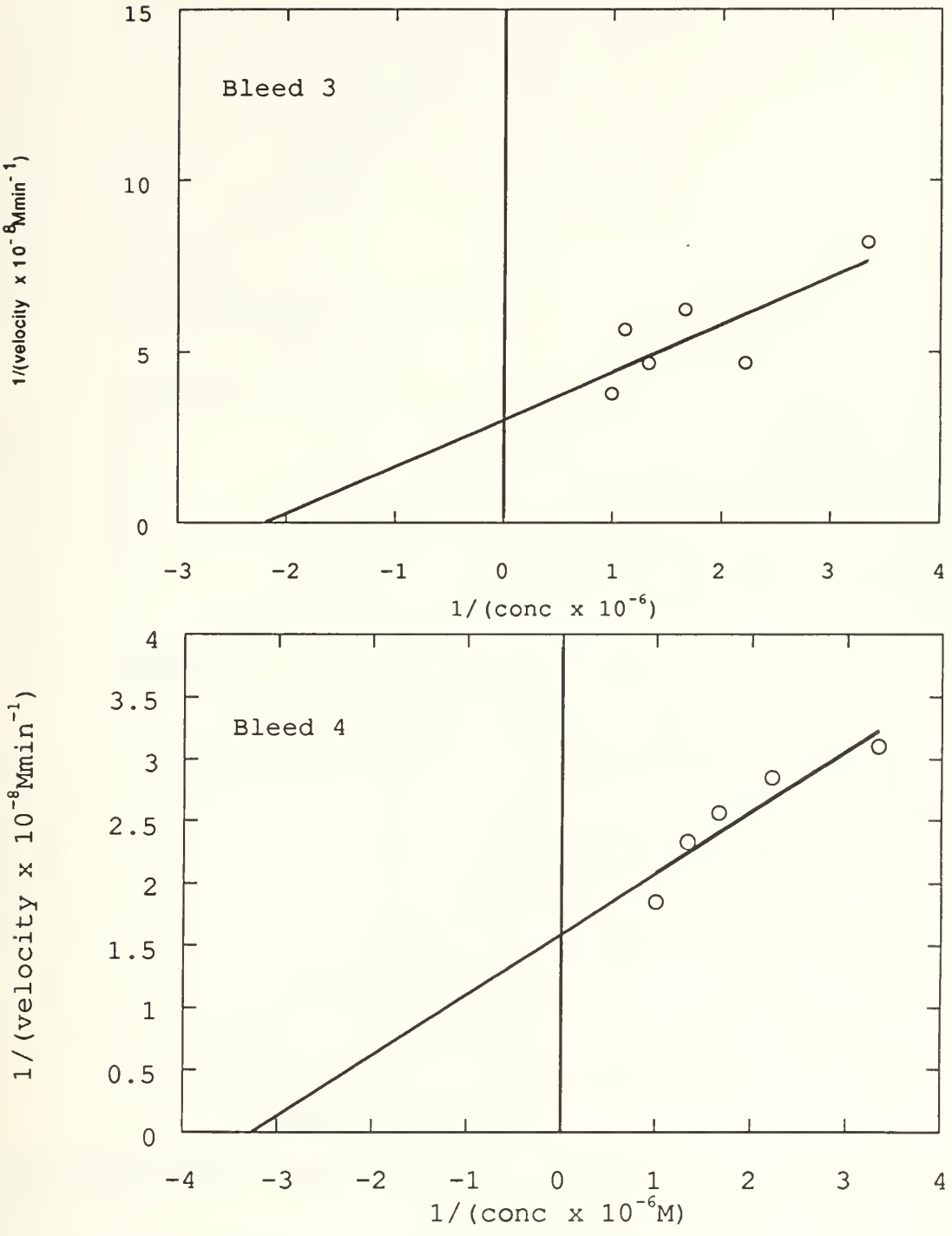


**Figure 12a**.Rabbit 2335 LWB plots.

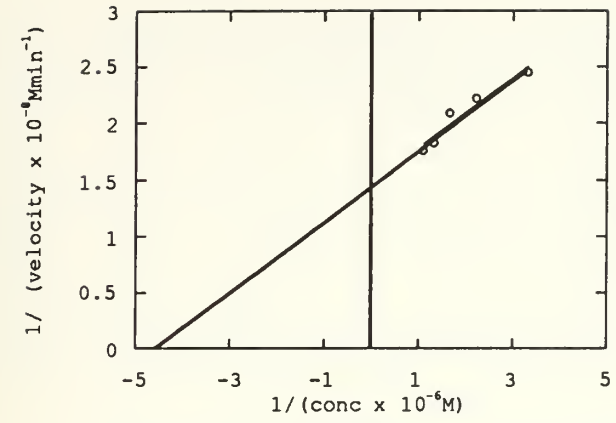


Bleed 2

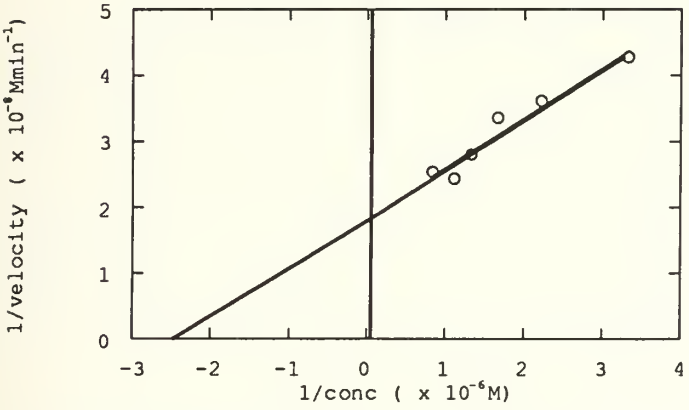


Bleed 3

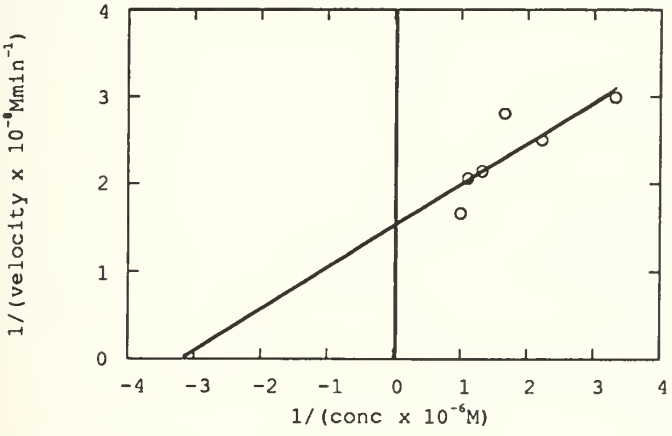


Bleed 4

**Figure 12b.** Rabbit 2336 LWB plots.

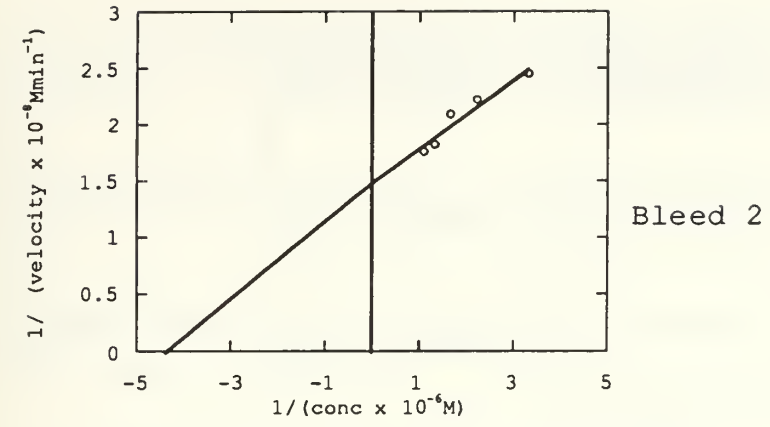


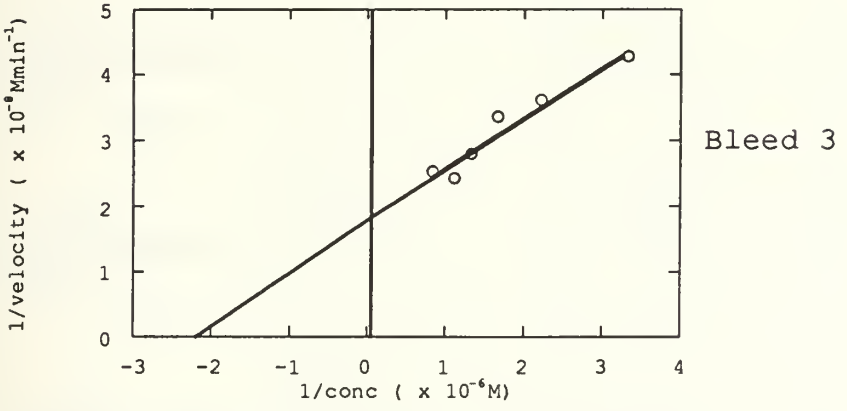


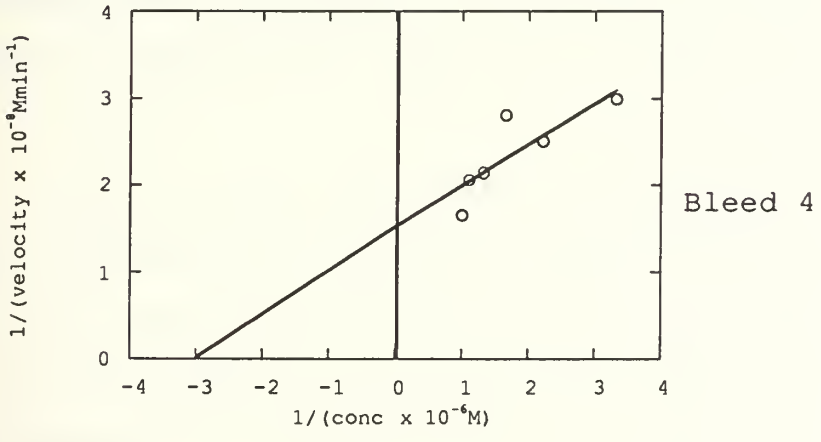


**Figure 12c.** Rabbit 2337 LWB plots.

| | Rabbit 2335 | Rabbit 2336 | Rabbit 2337 |
|---|---|---|---|
| Prebleed<br>$v_{max}$<br>$k_m$<br>Antibody Conc | None Detected | None Detected | None Detected |
| Bleed 1<br>$v_{max}$<br>$k_m$<br>Antibody Conc | None Detected | None Detected | None Detected |
| Bleed 2<br>$v_{max}$ (M/min)<br><br>$k_m$ (μM)<br>Antibody Conc | None Detected | $6.8 \times 10^{-8}$<br>($\pm 1.8 \times 10^{-8}$)<br>21 (±13)<br>1.0 mg/mL | $2.3 \times 10^{-7}$<br>($\pm 0.7 \times 10^{-7}$)<br>35 (±20)<br>1.0 mg/mL |
| Bleed 3<br>$v_{max}$ (M/min)<br><br>$k_m$ (μM)<br>Antibody Conc | $3.3 \times 10^{-8}$<br>($\pm 0.4 \times 10^{-8}$)<br>44 (±8)<br>0.5 mg/mL | $5.6 \times 10^{-8}$<br>($1.6 \times 10^{-8}$)<br>39 (±17)<br>0.1 mg/mL | $7.7 \times 10^{-8}$<br>($\pm 1.7 \times 10^{-8}$)<br>58 (±20)<br>0.1 mg/mL |
| Bleed 4<br>$v_{max}$ (M/min)<br><br>$k_m$ (μM)<br>Antibody Conc | $6.2 \times 10^{-8}$<br>($\pm 0.5 \times 10^{-8}$)<br>30 (±8)<br>0.5 mg/mL | $6.6 \times 10^{-8}$<br>($\pm 0.8 \times 10^{-8}$)<br>31 (±11)<br>0.1 mg/mL | $6.0 \times 10^{-8}$<br>($\pm 0.8 \times 10^{-8}$)<br>19 (±7)<br>0.1 mg/mL |

**Table 9**. Lineweaver-Burk results for the three rabbits.

Since our polyclonal samples are presumably a heterogeneous mix of catalysts, the values we obtained are then "apparent" values for the entire antibody population. These results show some interesting trends. As reported earlier Rabbit 2335 was "sick" throughout most of the study, and his parameters seem to reflect this fact. It can be seen that all three rabbits seem to show an increase in normalized velocity over the course of the 4

immunizations. It would also appear after a slight rise, their $k_m$ values decrease.

**Rate Enhancement and Catalytic Efficiency Determinations**. The ultimate goal of the catalysis studies is to show that the immune system is able to produce efficient catalysts which can significantly enhance the rate of a reaction. Rate enhancement is calculated by:

$$\text{Rate Enhancement} = k_{cat} / k_{uncat}$$

Where $k_{cat}$ or the catalytic constant is:

$$k_{cat} = v_{max} / [\text{Ab Binding Sites}]_T$$

and the concentration of antibody binding sites is:

$$[\text{Ab Binding Sites}] = [\text{Ab(M)}] \times 2 \times (\% \text{ Hapten Specific Antibodies})$$

The catalytic efficiency, or turnover number, is then $k_{cat}/k_m$. The values obtained for the catalytic parameters are given in Table 10. It was seen that the catalytic constant, $k_{cat}$, of the antibody increases over the course of the immunizations as did the catalytic efficiency. We can see that the catalytic parameters all increase throughout the immunization regimen, indicating a

refinement in the antibodies present to those of higher catalytic activity.

| | Rabbit 2335 | Rabbit 2336 | Rabbit 2337 |
|---|---|---|---|
| Bleed 2<br>$k_{cat}$ ($min^{-1}$)<br>Efficiency<br>Enhancement | None Determined | 0.26 (±0.07)<br>0.013<br>3,095 | 0.23 (±0.05)<br>0.006<br>2,738 |
| Bleed 3<br>$k_{cat}$ ($min^{-1}$)<br>Efficiency<br>Enhancement | 0.17 (±0.01)<br>0.004<br>2,023 | 0.62 (±0.10)<br>0.016<br>7,380 | 0.75 (±0.10)<br>0.013<br>8,928 |
| Bleed 4<br>$k_{cat}$ ($min^{-1}$)<br>Efficiency<br>Enhancement | 0.39 (±0.03)<br>0.013<br>4,643 | 1.27 (±0.15)<br>0.041<br>15,119 | 0.78 (±0.07)*<br>0.041<br>9,286 |

**Table 10**. Catalytic parameters for the catalytic samples. *$K_{cat}$ determined from after second purification. $K_{cat}$ determined from $v_{max}$ prior to second purification was 1.09.

## A: Discussion

**Monoclonal vs. Polyclonal Antibodies.** This study supports the feasibility of using catalytic polyclonal antibodies to investigate the maturation of the immune response. The entire study took only 4 months from inception to results. This is quite remarkable when compared to what would have been required for an analogous monoclonal study of the same scope and magnitude. The type of study described here will be easily be expanded to study the effects of slight variations in hapten size, complexity, stereochemistry, and structure on catalytic activity and efficiency. Furthermore, the results of these studies will be representative of the entire immune response, as are those obtained from this study.

**Antibodies are the Cause of Catalysis.** It was shown that the catalytic activity observed was not the result of some pre-existing antibody or enzyme. By verifying the lack of activity in the preimmunization samples, it was also shown that the catalytic activity seen is completely quenched by using the hapten as an inhibitor.

**Serum Titer as Catalytic Indicator.** The serum titer is not the most accurate indicator of catalytic activity. One can see from Table 11 that while the serum titer peaks and then drops after the third immunization, the catalytic activity and efficiency

continue to increase. We also see that the amount of hapten specific antibody present seems to correlate with the serum titer. This study seems to indicate that serum titer is representative of the amount of IgG antibodies present, but not necessarily an indicator of the quality of the catalytic antibodies.

| | Rabbit 2335 | Rabbit 2336 | Rabbit 2337 |
|---|---|---|---|
| Preimmunization Titer | <1/200 | <1/200 | <1/200 |
| Bleed 1 Titer | <1/200 | 1/1,200 | 1/1,536 |
| Bleed 2 Titer | 1/4,216 | 1/11,212 | 1/27,136 |
| $v_{max}$ x$10^{-7}$M/min | None detected | 0.68 (±0.18) | 2.3 (±0.7) |
| $k_m$ (μM) | None detected | 21 (±13) | 35 (±20) |
| %Active | None detected | 2.0 | 8.0 |
| $k_{cat}$ ($min^{-1}$) | None detected | 0.26 (±0.07) | 0.23 (±0.05) |
| Efficiency | None detected | 0.013 | 0.006 |
| Rate Enhance | None detected | 3,095 | 2,738 |
| Bleed 3 Titer | 1/28,800 | 1/32,000 | 1/51,200 |
| $v_{max}$ x$10^{-7}$/min | 0.66 (±0.08) | 5.6 (±1.7) | 7.7 (±1.7) |
| $k_m$ (μM) | 44 (±8) | 39 (±17) | 58 (±20) |
| %Active | 3.0 | 7.0 | 8.0 |
| $k_{cat}$ ($min^{-1}$) | 0.17 (±0.01) | 0.62 (±0.10) | 0.75 (±0.1) |
| Efficiency | 0.004 | 0.016 | 0.013 |
| Rate Enhance | 2,023 | 7,380 | 8,928 |
| Bleed 4 Titer | 1/9,600 | 1/30,720 | 1/22,016 |
| $v_{max}$(x$10^{-7}$M/min | 1.24 (±0.1) | 6.6 (± 0.8) | 6.0 (±0.6) |
| $k_m$ (μM) | 30 (±8) | 31 (±11) | 19 (±5) |
| %Active | 2.5 | 4.0 | 6.0 |
| $k_{cat}$ ($min^{-1}$) | 0.39 (±0.03) | 1.27 (±0.15) | 0.78 (±0.07) |
| Efficiency | 0.013 | 0.041 | 0.041 |
| Rate Enhance | 4,643 | 15,119 | 9,286 |

**Table 11.** This table is a summary of kinetic and catalytic parameters. $V_{max}$ values normalized to a 1 mg/mL value.

The importance of this point is that currently monoclonal antibodies are normally produced from animals showing the highest hapten specific titer. In our study, the highest $k_{cat}$ and rate enhancement was seen in rabbit 2, after his fourth immunization. All rabbits show the highest efficiency after the fourth immunization. Thus the titer measurement is not the best way to determine when, and which animal to use for monoclonal antibody production.

**Polyclonal Catalytic Antibody Variability**. This study again reinforces the idea that there is suprisingly little variability in the polyclonal antibodies produced by different animals of the same species. In this study Rabbit 2335 seemed to lag behind in his response. This is most likely a result of the fact that he was ill at the start of the study, i.e. the immune system of Rabbit 2335 was most likely preoccupied with some other problems. The health of Rabbit 2335 will be determined by a post mortem examination. In the 3 rabbits, after the fourth immunization, there was a 6 fold difference in $v_{max}$, a 3 fold variation in $k_m$, a 3 fold variation in percentage active antibodies, and a 3.3 fold variation in $k_{cat}$ and catalytic efficiency. If we exclude the sick rabbit, 2335, we see practically no variation in $v_{max}$, a 3 fold variation in $k_m$, and less than a 2 fold variation in $k_{cat}$ and catalytic efficiency. This is in line with the results seen in our previous studies (91-94). Once again,

polyclonal catalytic antibodies are able to provide an accurate depiction of the entire immune response and are reproducible.

**Rate Enhancements.** It is quite striking that the rate enhancements achieved by the polyclonal antibodies are essentially the same as those achieved by analogous monoclonal systems. Rate enhancements of ~$10^3$ to ~$10^4$ are consistent with those seen for similar monoclonal studies using phosphate haptens (41,75,93).

**Maturation of the Immune Response.** The kinetic and catalytic parameters obtained in this study are summarized in Table 11. The trends seen in these results indicate that over the course of the immunization regimen the catalytic efficiency of our polyclonal sample increases. There are two possible explanations. One possibility is that we are seeing better catalytic antibodies. The other possiblity is that we are seeing more of the higher affinity antibodies.

There have been studies in the past that have definitively shown non-catalytic-type antibodies display an increase in hapten affinity over the course of the immunization regimen. Figure 13 represents the results of a study in which multiple rabbits were immunized with a dinitrophenyl-BGG conjugate (31,86). There were four groups of multiple rabbits, with each group being immunized with a varying concentration of the antigen. In each case, the affinity of hapten specific antibodies increased over the course of a 6 week period following immunization. A similar study using

guinea pigs, immunized with the same hapten, showed the same results. The results are represented in Figure 14 (43). A substantial increase in antibody affinity for hapten is seen over the period of 2 months following immunization. There are numerous other studies reporting similar trends (13,22-26,33-35).

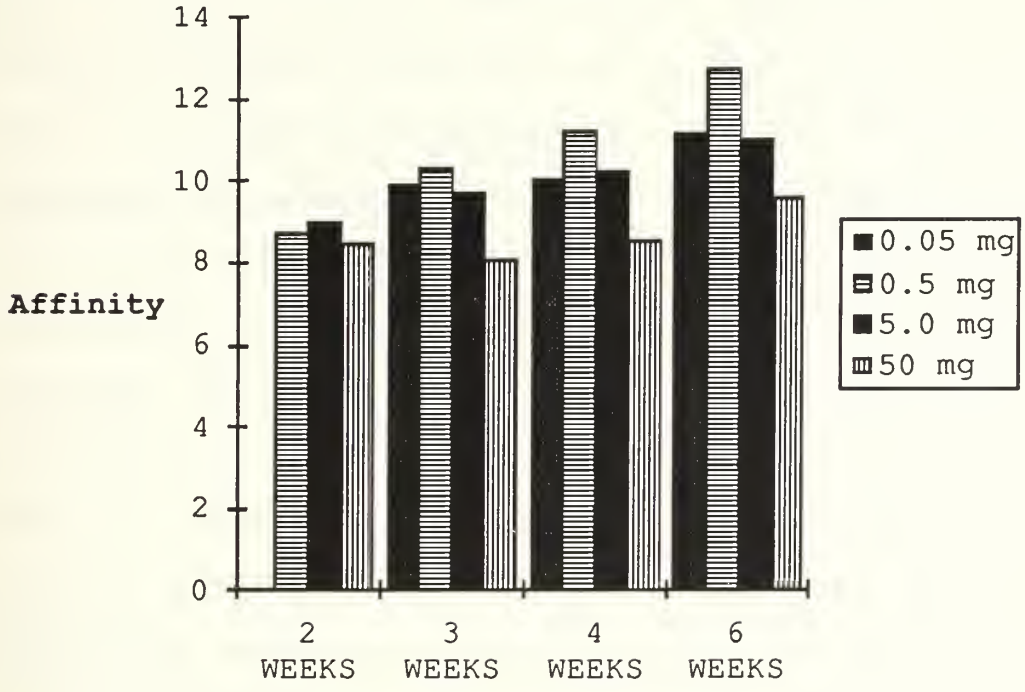


**Figure 13**. The maturation of antibody affinity as seen in rabbits immunized with 2,4-dinitrophenyl-BGG. The affinity was measured by fluorescence quenching with e-DNP-L-lysine. Affinity is in kcal/mole.

This study shows a definite increase in catalytic efficiency through the first four immunizations. This study shows that the immune response is still optimizing after 4 immunizations. There is also a continued increase in catalytic efficiency.

Let us look at Rabbit 2337. We see the $k_{cat}$ was 0.23, 0.75, and 0.78 after the second through fourth immunizations respectively. The rate enhancement was 2738, 8928, and 9286. This would seem to indicate the immune response may have reached its peak. However, we see $k_m$, which reflects substrate binding for catalytic antibodies, decrease to 19 μm, from a high of 58 μM, which is of limited significance. We also see that catalytic efficiency has increased from 0.006 after second immunization, to 0.013 after third immunization, to 0.041 after the fourth immunization. The immune response of Rabbit 2337 is still optimizing after four immunizations. Thus, as stated in the introduction, in order to see an increase in catalytic efficiency, with no corresponding increase in rate enhancement, the only possible explanation is that there was a similar increase in the stabilization of both the transition state and the substrate, which is case 6 of Table 3.

One can infer that our phosphate hapten, with its tetrahedral geometry and negative charge, accurately mimicked the tetrahedral intermediate in the hydrolysis of the carbonate substrate. The closer the hapten mimics the transition state, the higher the catalytic activity should be in the antibodies. The binding and stabilization of the tetrahedral intermediate in this case apparently lowered the energy of activation for the carbonate hydrolysis. This would subsequently enhance the rate of hydrolysis.

This is wholly consistent with the notion that an increased affinity to hapten causes increased stabilization of the corresponding tetrahedral intermediate.

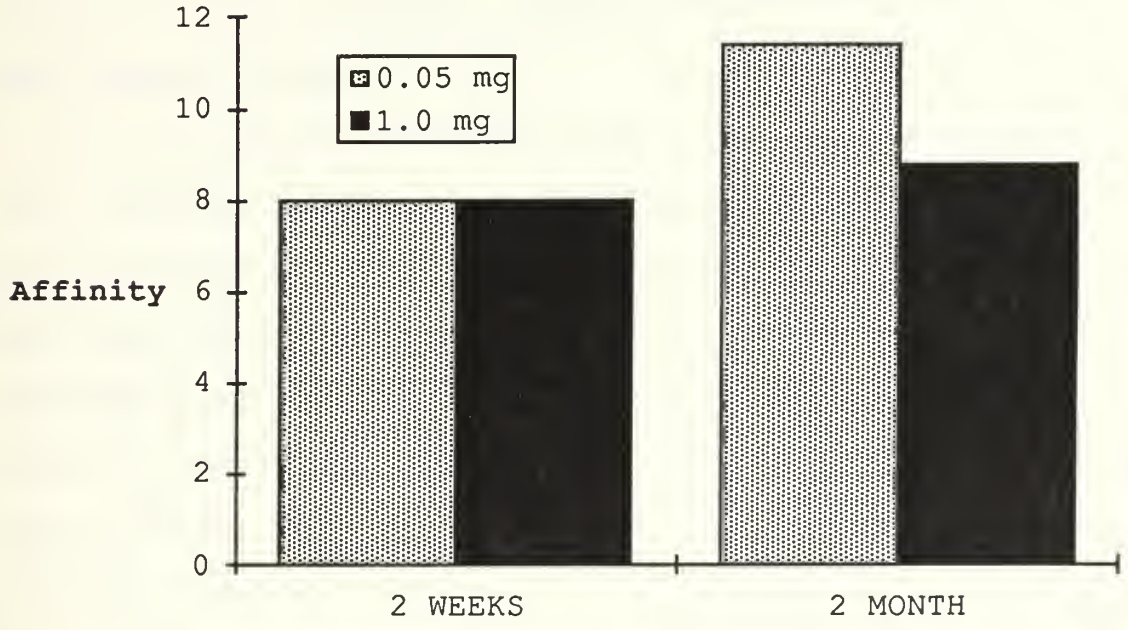


**Figure 14**. The maturation of antibody affinity as seen in guinea pigs immunized with 2,4-dinitrophenyl-BGG. The affinity was measured by fluorescence quenching with e-DNP-L-lysine. Affinity is in kcal/mole.

There can be no argument that catalytic polyclonal antibodies are produced by the immune system of the rabbits, not by the researchers. We are still presented with the question of whether the immune system possesses all the required machinery or whether it evolves its response over the course of an immunization. There is no doubt that the catalytic activity elicited in this study

showed a remarkable increase over the course of this study. Choosing a correct tetrahedral intermediate mimic does have an effect on the catalytic activity. This will be further probed by extensive studies in the near future. These results cannot be a purely genetic phenomenon.

The clonal selection theory seems to be a valid explanation here. This study does show that over the course of our immunization we see catalytic activity increase as the amount of hapten specific antibodies decreases. Therefore, it is probable that as the immunization proceeds, the antibody producing cells with highest affinity are selectively stimulated resulting in production of the higher affinity antibodies. The higher affinity antibodies thus proliferate later in the response.

The results of this study and our previous variability study, seem to indicate polyclonal antibodies show a tendency towards a homogeneous response. The idea that seems to be most logical is a combination of theories. Do all animals of a species start with a similar germ line? The high affinity antibodies produced as the immune response matures probably contain related amino acid sequences in their binding pockets. The antibody producing cells all start with a set of restricted germ line variable region genes. The slight variation seen between unrelated animals may be due to somatic recombination in the variable region of their genes. If the

hapten used is not the best mimic of the tetrahedral intermediate, the catalysis seen will be less than optimal.

The one piece of data we could not measure directly, due to time constraints and technical difficulties, was the apparent affinity or exact composition of the polyclonal antibody response. There is currently a joint research project being conducted with the Whitesides' group at Harvard, the goal of which is to show the distribution of affinities in polyclonal sera. This method will employ capillary electrophoresis, and may be on-line by the end of the summer.

## A: Conclusions

Polyclonal antibodies have proven to be an effective method for studying the maturation of a catalytic immune response. Therefore, polyclonal studies shall also allow complete and systematic studies of the optimization of hapten and antigen design. The advantages of this complete, comprehensive, and resource effective method can no longer be ignored.

The most important trend uncovered here is there is a tendency towards homogeneity of the catalytic immune response after repeated immunization. Antibody affinity for the tetrahedral intermediate is presumed to increase over the immunization regimen. It is known from previous studies that repeated immunization results in increased antibody affinity. This increase in antibody affinity presumably results in an increase in catalysis. Since the immune system does not purposely evolve to optimize catalytic activity, the affinity for the tetrahedral intermediate must incrase over the immunization regimen to see an increase in catalytic activity. This means the simple binding model of catalytic antibodies is probably correct. We are assuming that the increased affinity for hapten stabilizes the transition state to a greater extent than the ground state, as affinity increases. Thus, we believe that the higher affinity antibodies that are encouraged

to dominate the immune response with repeated immunizations are the best catalysts. These catalytic antibodies may also prove to contain point mutations which improve catalytic activity. The actual affinity and affinity distribution of these polyclonal antibodies shall be measured as soon as an accurate technique becomes available.

Was Rabbit 2337's immune response optimized after the third immunization? The titer had dropped after the fourth immunization. The rate enhancement and $k_{cat}$ do not change. However, $k_m$ has dropped, indicating better substrate binding. The catalytic efficiency has also increased, thus the only possible explanation is that there is an increased stabilization of both the substrate and the tetrahedral intermediate. Rabbit 2337's immune response is still optimizing after the fourth immunization!

Let us again emphasize the point that it is not readily apparent that antibodies should be catalytic. The fact is that antibodies evolve over the course of the immunization regimen to bind more tightly to the hapten. The fact that catalysis occurs is thus an artifact of binding to the tetrahedral intermediate. This is quite extraordinary. The fact is that the more closely we can mimic the intermediate of a reaction, the lower the energy barrier becomes, and the higher the catalytic activity seen.

The rabbits used in this study will continue to be immunized and studied, to further examine the long term immune response

maturation. We predict that the immune response will continue to optimize its catalytic activity through increased affinity. We should see the affinity for substrate plateau at a relatively low value, followed by the catalytic activity reaching some constant value. We do not believe these rabbits have optimized their immune responses yet, but after several more immunizations, their antibodies should reach a peak, stable catalytic activity level. The study will be terminated when the immune response reaches a stable catalytic level.

Polyclonal antibodies provide us with a unique opportunity to examine the entire immune response, as opposed to the limited view presented by monoclonals. Let us go back to our needle in the haystack analogy. Polyclonals will allow us to first of all ensure we are searching in the right haystack. They will then allow us to significantly reduce the magnitude of our haystack, and find the needle with the sharpest point. Polyclonals will revolutionize the way we think about catalytic antibodies.

## A: Experimental

**Materials and Methods**. All chemicals were of reagent grade quality, and purchased commercially. They were used without further purification.

ELISA readings were conducted on a Bio-Tek Instruments microplate reader (EL 311). Analytical HPLC studies were performed on a Hewlett-Packard 1090M liquid chromatograph with a HP 8452A diode array detection system and a HP 79994A analytical workstation. $^{1}H$ NMR data were obtained on a General Electric QE-300 MHz instrument.

Preparative low pressure chromatography was done using a HR 10/10 column filled with Gamma Bind Protein G-Sepharose (Pharmacia LKB) using a Pharmacia LKB fast protein liquid chromatograph (FPLC), with 2 P-500 pumps, a GP-250 controller, and UV-2 dual path monitor.

Three 5 pound heterozygous male New Zealand white rabbits were obtained from R&R Rabbitry, Pipe Creek, Texas.

The reaction buffer used in all studies was 10 mM Tris buffer.

**Preparation of Protein Conjugates**. Hapten (12.0 mg, 0.0216 mmol) and KLH (20.0 mg) were placed in 2.0 mL 1xPBS; N-hydroxysulfosuccinimide (8 mg, 0.0369 mmol) and [1-ethyl-3-(dimethylamino)propyl]-carbodiimide (12mg, 0.0625 mmol) were added. The mixture was stirred for 60 min at room temperature. The conjugate was dialyzed against 1xPBS buffer (3x) for 3 days. This solution was diluted to 1 mg/mL (protein concentration, and stored at -20 $^{o}$C. The same conjugate was used to prepare ELISA plates.

**Rabbit Immunizations**. Three 5 pound male New Zealand rabbits were bled as a control. A mixture of 0.5 ml hapten-KLH (1 mg/mL) and 0.5 mL Freund's complete adjuvant was prepared. Seven days later each of the 3 rabbits was subcutaneously injected with a 1 ml mixture on the dorsal surface between the shoulders. The injection was administered in 3 to 4 different spots. Subsequent injections used Freund's incomplete adjuvant. The rabbits were immunized at 21 day intervals. Bleeds of about 10 mL were conducted 10 days following each injection.

**Antibody Isolation and Purification**. The whole blood was immediately separated into cells and serum by centrifugation at 10,000 g for 10 min. The serum was separated and stored overnight at -20 $^{0}$C, and the cells were discarded. The serum was thawed. Two volumes of 60 mM sodium acetate, pH 4.0, was slowly added to the serum while stirring. The pH was adjusted to 4.8. While continuing to stir, 0.75 mL caprylic acid per 10 ml of serum was added dropwise. The mixture was shaken for an additional 30 minutes. The solution was then centrifuged at 5000 g for 10 min. The supernatant was decanted and placed in 50,000 molecular weight cut-off tubing (MWCO), and dialyzed overnight against three

changes of 10 mM Tris, at 4 °C. The dialyzed samples were then mixed with an equal volume of saturated ammonium sulfate while slowly stirring. The solution was then allowed to stand at 4 °C overnight (≥6 h). The mixture was then centrifuged at 3000 g for 30 minutes. The supernatant was decanted and discarded. The white pellet was suspended in 0.3 to 0.5 volumes of Tris buffer. The dissolved pellet was then loaded into 50,000 MWCO dialysis tubing and dialyzed overnight, at 4 °C, against 3 changes of Tris buffer. The solution was centrifuged at 3000 g for 10 min to remove any debris. The samples were then purified on a HR 10/10 column filled with Protein G-Sepharose 4 Fast Flow using an FPLC system with ImmunoPure Binding and Elution buffers. The purified samples were neutralized with Tris buffer. The samples were then concentrated by ultrafiltration. The samples were again dialyzed, in 50,000 MWCO tubing, against 3 changes of Tris buffer overnight, at 4 °C. The concentrations of purified IgG were determined by absorbance at 280 nm. The purified samples were kept at -20 °C when not in use.

**Preparation of ELISA Plates.** The hapten-KLH conjugate was diluted 1:500 in Tris buffer, and 25 mL added to each well of a 96 well low affinity ELISA plate. The plate was then placed at 37 °C overnight.

**ELISA-Titer Determination.** The hapten-KLH was fixed onto the plate by placing 50 µL of methanol into each well and allowing to stand 10 min. The methanol was removed and the plate air dried. To each well, was added 50 µL of a BSA solution (1 mg/mL) in Tris. The plate was stored in a moist chamber at 37 °C for 1 h. The BSA solution is removed and 25 µL of the same BSA solution is added to each well except those in the first column. To the first well in each row, is added 50 µL of a solution of 1:100 antibody sample. The antibody sample was then serially

diluted by taking 25 µL from the first row and transferring it to the next well and mixing thoroughly. This procedure was repeated across each row from well 1 to 12. The plate was then stored in a moist chamber at 37°C for 4 hours. The plate was then rinsed 10 times in a stream of water. A secondary antigen of Goat-anti rabbit was diluted 1:500 and 25µl added to each well. The plate was placed in a moist chamber at 37 °C for 1 hour. The plate was rinsed 10 times in a stream of water. To each well was then added 50 µL ABTS. The plates were read at 5 and 15 minutes. The readings were then averaged.

**Catalytic Assays.** The catalytic assays were carried out in 20 µL volume reactions. The reactions contained 18 µL of a premixed antibody solution, and 2 µL of a substrate solution. The antibody and substrate solution were diluted with 10 mM Tris buffer as necessary. Substrate concentration in the reactions varied from 30 to 150 µM. The background hydrolysis rate was determined in the absence of antibody. The reactions were incubated at 25 °C for 1 to 7 h, and then immediately analyzed by HPLC. All reactions were run for 10-30 % product conversion and were repeated in triplicate. Lineweaver-Burk analysis was done to determine $v_{max}$ and $k_m$. The standard deviation was determined by plotting the three sets of data separately for each rabbit and bleed. Standard deviations calculated using the following equation.

$$S = [S(x_i - x_{ave})^2/N-1]^{0.5}$$

The reported Lineweaver-Burk data is that extracted from the plots of the average of three data points. The error in the integration of peaks is ±5 %.

**HPLC Analysis.** The samples were injected onto a 4.6 mm X 15 cm Vydak $C_{18}$ column with a Vydak $C_{18}$-filled precolumn. The elution

conditions consisted of a flow rate of 0.7 mL/min of 40 % methanol /60 % $ddH_2O$ for 6.0 min, followed by a 0.2 min ramp up to 70 % methanol, after 3 min, a 0.20 min ramp down to 40 % methanol. The reaction products consisting of the phenol and the 4-(butylamide) benzyl alcohol eluted at about 5 and 6 min respectively. The starting substrate eluted off at about 11.7 min. Products were identified by coinjection with known compounds. Reaction rates were determined by peak integration. The conversion to product was determined by integrating the product peak at ~ 6.0 min, and dividing by the sum of the integration of itself and the substrate peak at ~ 11.5 min. The integrations were done at 235 nm. The phenol peak existence was verified at 210 nm.

**Background Rate Determination.** The background rate was determined in reaction buffer, and in reaction buffer in the presence of prebleed serum. A solution of 150μm substrate was allowed to stand for 2 days at 25°C. The reaction mixture was analyzed for conversion of substrate to product by HPLC.

The background was also determined in the presence of prebleed sera. The reactions consisted of 16-19 μM antibody from the prebleed, and 150 μM substrate. The reactions were allowed to go for 2 days. The reactions were analyzed by HPLC.

Background rates were determined from the following equation:

$$\text{Background Rate} = k_{uncat} = \{- \ln [s]_f/[s]_i\}/\text{time(min)}$$

**Prebleed Serum Activity.** To verify the lack of catalytic activity present prior to immunization, catalytic assays using prebleed serum were conducted. The reaction volumes were 20 μL. The reaction

consisted of 150 μM substrate and 16-19 μM serum. A second set of reactions included 16-19 μM inhibitor. The reactions were incubated for 8 to 9 h at 25 $^{o}$C. The reactions were then analyzed by HPLC.

**Inhibition Analysis:** Reaction solutions were each 20μL. They consisted of 16 μL of antibody solution, and 2 μL of a hapten solution of varying concentrations. The hapten concentration was varied from 0 to 20 % of the antibody binding site concentration. The antibodies were incubated with the hapten for at least 18 min. Then 2μL of substrate was added to bring the substrate concentration to 150 μM. After 18 min at 25 $^{o}$C, the reaction were analyzed by HPLC. All reactions were run for 10-20 % product conversion. The results for each individual sample were plotted as fraction of substrate converted versus percentage of hapten. A straight line was drawn through the points. The point where the line intercepts the x axis is considered the percentage of active antibodies.

**Determination of Theoretical Inhibition Plots.** The math program *Mathematica* Version 2.2 (Wolfram Research) was utilized for this analysis. The program was allowed to solve a series of five equations, with five unknowns, for a general solution. The solution would be for the concentration of antibody bound substrate, or Ab-S. Known values were inserted for the antibody concentration, the substrate concentration, and $k_m$, and the program was then allowed to come up with a simplified equation for Ab-S. Then the equation was solved for values of $k_h$. The values used for $k_h$ were 0.00001, 0.0001, 0.001, 0.01, 0.1, 0.99, 10.0, and 100.0. Into each equation obtained for various values of $k_h$ were plugged values for hapten from 0.0 to 30.0 mM. The values obtained for Ab-S were normalized and plotted against normalized values of hapten. The eight curves (one for each value of $k_h$) were compared to

an actual normalized inhibition plot to validate the characteristics of the curve seen, and get an estimate of the actual $k_h$.

## B: Research Objectives and Aims

The research described in this thesis gives us a better understanding of the molecular recognition properties of the sapphyrin-type expanded porphyrin. It has been discovered in our labs that the sapphyrins have the ability to selectively recognize and bind anions(94-98). By attaching sapphyrin molecules to a chromatographic support, one can further probe the interactions between various anions and the sapphyrin. This work shows the feasibility of using expanded porphyrins, specifically the sapphyrin class, as a chromatographic support for analyzing and purifying mixtures of anions, such as phosphates. This study focuses on the development of a sapphyrin-modified silica support for use in HPLC analysis.

The ability of sapphyrins to bind DNA through phosphate chelation led us to realize that a sapphyrin-bound silica gel could be used to separate oligonucleotides as well as DNA and RNA fragments. Sapphyrin binds to DNA with a high affinity, showing a $K_a$ of $2.5 \times 10^4$ $M^{-1}$(99). This could provide a tool for use in purification of synthetic oligonucleotides, and nucleic acids. The ability of sapphyrin-based chromatographic supports to recognize and bind other anions of interest will also be investigated.

In a less successful project, a sapphyrin dimer was proposed in order to enhance our understanding of the interaction of

sapphyrin and DNA in solution. Since it has been proven that sapphyrin is able to bind double stranded DNA(99) in solution. It would be interesting to find out whether a conjugate with two sapphyrins will show enhanced binding to DNA.

## B: Background and Significance

**Sapphyrin.** Sapphyrin **1** is a pentapyrrolic expanded macrocycle, which belongs to a group of molecules referred to as expanded porhyrins **2** (100). It was first reported by Woodward and coworkers (101,102), who discovered it while attempting to synthesize vitamin B-12.

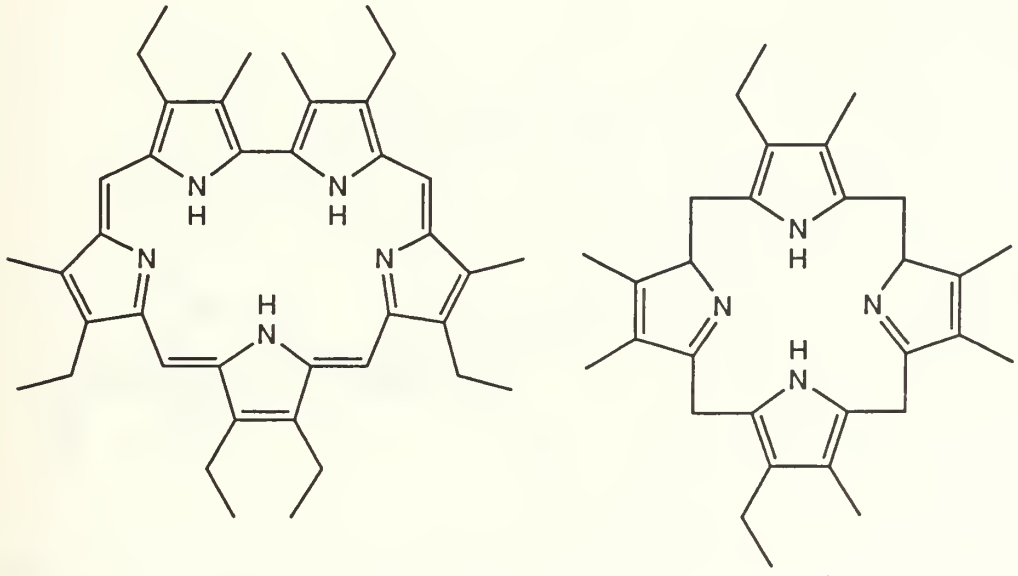


1 2

**Figure 15.** The basic structure of sapphyrin and porphyrin.

The sapphyrin macrocycle is monoprotonated at neutral pH (99). Thus, the interior of the sapphyrin macrocycle forms a large basic cavity (95,103,104). The four protons present in the monoprotonated core are capable of forming strong hydrogen bonds to

select anions such as fluorides and phosphates, in both solution and solid state (105,106).

Sapphyrins have been shown to possess unique molecular recognition properties towards certain anions (94-96,103-109). Due to the nature of these reactions, they represent the chelation of the anions by the protonated core. A crystal structure of the diprotonated form of sapphyrin showed it chelating a phosphate anion, see Figure 16 (96).

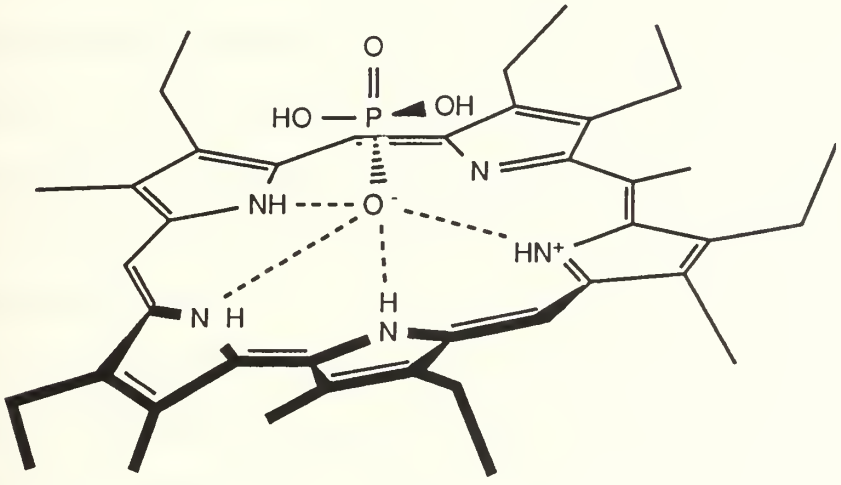


**Figure 16.** Representation of the X-ray crystallographic structure of the 1:1 complex formed between the monoprotonated sapphyrin macrocycle and phosphoric acid.

The ability of sapphyrin to chelate to the phosphate backbone presented a unique DNA-small molecule interaction that was discovered by Shreder of our group (99). The initial evidence for this interaction was the result of mixing an excess of water

soluble sapphyrin **1**, which in solution is a deep emerald green color, to double stranded DNA at neutral pH. The result was an immediate precipitation of green fibers. The results of solid state $^{31}P$ NMR analyses further support this event as being a chelation interaction (110).

UV-Visible studies were used to calculate an apparent binding constant of $2.5 \times 10^4$ $M^{-1}$ for sapphyrin to single stranded DNA (99). The results seen for the case of sapphyrin to double stranded DNA yielded similar spectral shifts, but the calculations were more complex. The spectral shifts could be the result of more than one interaction in solution. The sapphyrin, which is known to aggregate in solution, may be aggregating at high sapphyrin to DNA concentrations.

The possibility that sapphyrin was intercalating was ruled out by studies with Topoisomerase I (111). In the presence of sapphyrin, dsDNA was not unwound by Topoisomerase I. This indicates that intercalation was not the mode of interaction. Thus, this type of interaction is referred to as phosphate chelation.

**Modified Solid-Supports.** Cram (112) and others (113-118) have demonstrated that the attachment of a molecule to a solid support may yield insights into the nature of the receptor (solid support attached)-substrate interactions. This approach allows binding interactions involving a large number of substrates to be rapidly analyzed, under identical experimental conditions. Thus,

receptor molecules can be quickly evaluated to determine their potential for use in new or improved chromatographic supports.

Chromatographic methods can be designed to exploit specific receptor-substrate interactions. The result is the ability to define subpopulations of molecules (119). This idea of using a receptor ligand covalently attached to a solid support is sometimes referred to as affinity chromatography. In HPLC applications, this is called High Performance Affinity Chromatography (HPAC) (120).

The macrocyclic polyethers known as crown ethers have shown the ability to form complexes with cations (121). There are many examples of functionalized crown ethers being covalently attached to solid supports for use in ion chromatography (115).

As an example, Cram reported that a crown ether receptor molecule covalently attached to a solid support was able to optically resolve amino acids and ester salts (112). In this case, a large optically active crown ether was covalently attached to cross-linked polystyrene-divinylbenzene resin. The resultant resin (Figure 17) was packed into a chromatographic column.

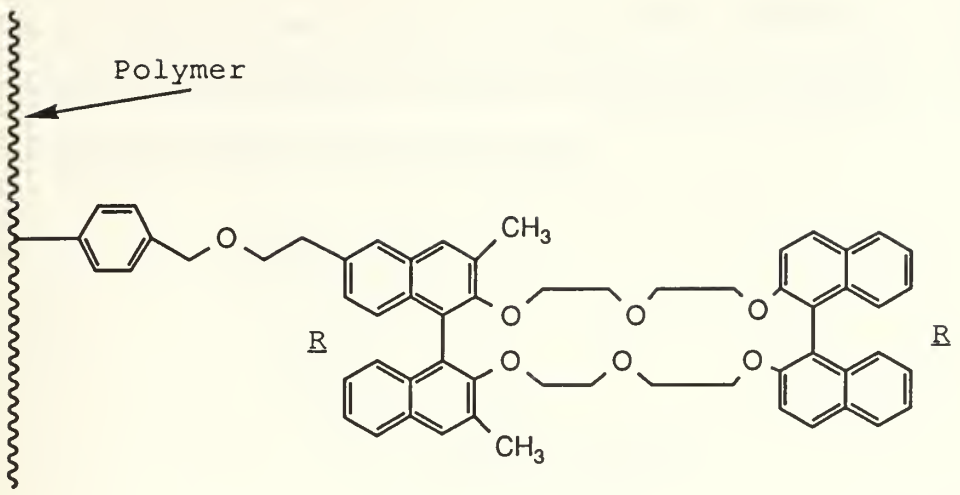


**Figure 17.** Solid support synthesized by Cram for optical resolution of amino acids and peptides.

The practice of preparing silica-bound macrocycles has been greatly expanded by the works of Bradshaw and Izatt (113,114,122). Silica-bound aza-crown and poly-aza crown macrocycles were used to probe crown molecule selectivity towards metal ions. The stable silica-bound macrocycles were able to be used in multiple studies, while preserving the precious macrocycles. It was also discovered the bound macrocycles showed selectivities and binding properties similar to those seen in the unbound macrocycles.

Schilde and Uhlemann reported the use of a special chelating type resin for separating oxyanions (123). The chelating resin was produced by the reaction of chloromethylated styrene-divinylbenzene polymer with an amino sugar, 1-deoxy-1-(methylamino)-glucitol groups (Figure 18). The two hydroxyl groups in the *cis* position

were able to form certain oxyanion diol complexes. Selective separation of aluminate, gallate, germinate, plumbate, vanadate, and molybdate from brines were seen.

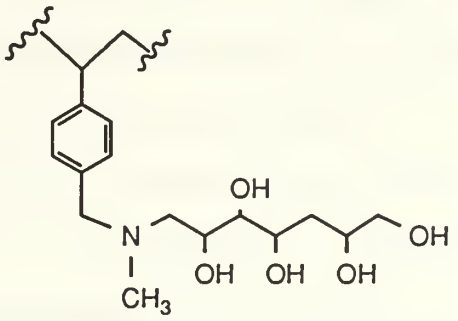


**Figure 18**. Methylamino-glucitol groups of the special chelating resin.

There are many examples of metal-porphyrin complexes being incorporated into solid supports (124). Kokufuta *et al.* reported the use of chloromolybdenum (V) tetraphenylporphyrin complex containing polymer as an anion exchanger (118). The solid supports were then submersed in a solution containing phosphate ions. The concentration of anions in solution was measured. The porphyrin complex showed a slight preference for the phosphate anion over the chloride anion.

Meyerhoff and coworkers have done extensive investigation into the anion selectivity of various types of porphyrin complex-modified solid supports (117). They prepared and characterized covalently bound porphyrin-silica gel stationary phases, with tetraphenyl porphyrin covalently attached to silica gel. The

porphyrin was subsequently metalated with either tin (IV) or indium (III). By varying the metal in the core of the porphyrin, the selectivity of the modified-silica gel was modified for aromatic anions. This indicates the metal in the macrocycle is capable of coordinating with anions in solution.

Meyerhoff and coworkers have also investigated the anion selectivity of potentiometric response of poly(tetrakis(p-aminophenyl)porphyrin) film-modified electrodes (116), the thiocyanate selectivity of Mn (II)-porphyrin-based electrodes (124), and the potentiometric anion selectivity of polymer membranes doped with Indium (III)-porphyrins (125).

**Separation of Biologically Relevant Molecules.** HPLC and other solid supported chromatography methods are finding increased usage in the separation, purification, and analysis of phosphorylated species such as nucleotides, oligonucleotides, DNA and RNA fragments, anti-viral treatments, pharmaceuticals, environmental contaminants, and chemical warfare agents.

A variety of new separation techniques, as well as modifications of existing techniques, have been recently developed (126). Many of these techniques prove to be expensive and quite often inefficient. Efficiency is a paramount concern, as the separation of compounds in pharmaceutical and certain biotechnology industries must show greater than 99.9 % purity (sometimes > 99.99 %), while delivering high yields (126).

Natural sciences have turned to HPLC as a preferred method for the separation and analysis of biological molecules. There have been many reports detailing the use of HPLC (127-132). They include the use of silica phases with bonded groups, such as linear hydrocarbons, amino and cyano-groups, carboxylic amides, amino acids, etc. (127-132). Researchers still commonly use radio-labeling and gel electrophoresis (GE) in cellular and synthetic oligonucleotide purification and analysis. The methods of GE and radio-labeling can be relatively time-consuming, painfully manpower intensive, and low yielding (133,134). Thus, an improved method for separating these types of molecules would have significant value.

The importance of being able to efficiently purify synthetic oligonucleotides is obvious. Synthetic oligonucleotides have a broad range of applications in biotechnology. The applications include providing templates for carrying out deletions, additions, and site specific mutagenesis, acting as adapters for cloning, and performing construction of genes. In the areas of interest that are currently being monitored by the US Food and Drug Administration (FDA), are probes for the detection of genetic diseases, probes for the detection of the provirus of Acquired Immunodeficiency Syndrome (AIDS), cloning techniques used for the treatment and diagnosis of infectious diseases, and purification and analysis of modified synthetic oligonucleotide chemotherapeutic agents (135).

Takemoto *et al.* recently proposed an alternate separation technique. It employed bonding purine and pyrimidine bases on the surface of silica gel (136). This approach improved separation of nucleic acids by base pairing interactions with their silica-bound nucleic acid base pairs. Takemoto *et al.* showed such stationary phases could be used to separate nucleic acid free bases, purine alkaloids, nucleosides, nucleotides, and oligonucleotides.

Separation of nucleotide mono-, di-, and triphosphates from cell extracts have often been problematic. The ability to separate the adenylate mono-, di-, and triphosphates is in itself instrumental in determining cell energy charge. The cell energy charge is given by:

$$\text{Adenylate Energy Charge} = \{[ATP]+0.5[ADP]\}/\{[AMP]+[ADP]+[ATP]\}$$

The energy charge is used as a determination of cell health in the study of many diseases (137,138).

Ion exchange HPLC columns for separating nucleotides and oligonucleotides already exist. Some of these columns utilize a bonded silica phase that operates by a weak anion exchange principle, and provides modest separations of nucleotides of up to 30 residues and other small molecules. There are several different bonded silica phase HPLC columns available that utilize a strong anion exchange principle to provide limited separation of

nucleotide monophosphates. There are also several utilizing a strong cation exchange interaction to separate nucleic acid bases. In the area of synthetic oligonucleotide separations, there are HPLC columns available that can on a limited basis separate oligonucleotides of 40 residues or less. Many of these columns are severely limited in their range of applications or in some cases require harsh conditions. For example, Diethylaminoethyl (DEAE) systems are able to achieve separations of nucleotides and oligonucleotides with good purity, but require a pH as low as 2.0(139).

The main disadvantages in using HPLC are lengthy analysis times and a lack of high efficiency in the analytical mode(140). There are also often inadequate yields in preparatory modes. The use of high-performance capillary electrophoresis (HPCE) shows promise in analytical modes. HPCE is one of the most significant bioseparation tools developed in the past twenty years. It is a highly sensitive analytical method capable of providing the rapid and efficient separation of a variety of species from complex mixtures 141). HPCE has shown promise in the analysis of pharmaceuticals, amino acids, proteins, nucleotides and DNA. The work of Zare *et al.* has shown great promise in the analysis of cell profiles of human peripheral blood lymphocytes and Molt4 human leukemia cells in the study of intracellular metabolism of nucleotides relating to the understanding of AIDS (138). The main

disadvantage of HPCE is that it is limited to small scale analytical separations.

A focus of research in our labs is the synthesis and study of expanded porphyrins (100,106,142). It was found the sapphyrin macrocycle exhibits unique molecular recognition properties towards anions (143). Recent attention has focused on the binding of biologically important phosphate species. Nucleobase substituted sapphyrins showed selective transport of monophosphates at physiological pH. The interaction of sapphyrin with DNA, which we have termed phosphate chelation, displays a mode of binding not previously seen in porphyrin chemistry (99). This presents the possibility of practical medical and biotechnological applications (96).

**Environmental Concerns.** Environmental concerns are taking center stage in all of our lives. Chromatography proves to be one of the most important methods for analyzing for pesticides, herbicides, fungicides, and their primary hydrolysis products (144-148). Many pesticides contain organophosphorous compounds. Organophosphorous compounds are known to inhibit acetylcholinesterase in mammals (149). It would be significant to develop better methods to analyze ground water, soil, food stuffs, etc., for contaminants such as the pesticides Dichlorovos, Phosphamidon, Diazanon, and Parathion.

**Chemical Weapons.** The end of the Cold War has left the United States and the former Soviet Union with large stockpiles of chemical warfare agents. Third World nations such as Libya and Iran are turning to this relatively low technology, but extremely devastating weapons of mass destruction. Some of these chemical warfare agents, such as Sarin, and their primary hydrolysis products are organophosphorous compounds. The magnitude these problems are self-evident (150-152).

Our sapphyrin-substituted silica gels may allow for detection and analysis of these noxious agents, and their primary hydrolysis products. This, in turn, would allow one to deal with disposal in those cases where they are present.

**Sapphyrin Dimer.** A second, different sapphyrin project was also carried out. It has been shown that sapphyrin binds to double stranded DNA in solution (99). We are interested in seeing if a second covalently attached sapphyrin would greatly increase the affinity for double stranded DNA. It has proven difficult to spectroscopically show the binding constant of sapphyrin to dsDNA, therefore an Fe (II)-EDTA type entity will be covalently attached to the sapphyrin dimer to effect cleavage of the DNA. Fe (II)-EDTA is known to cleave DNA (153,154), and thus we will be able to compare the effect of a second covalently attached sapphyrin on an already studied system (99).

**Overall Significance**. The most significant goal of this research is to demonstrate the feasibility of using solid supported macrocycles to further investigate their binding specificity.

## B: Results

**Synthesis of the Sapphyrin-modified Silica Gels.** The sapphyrin modified gels were synthesized by an amide coupling, as shown in Figure 19. These synthesis were performed by Kral in our labs. The gels were then custom packed into 4.6 mm x 10cm columns by ALLTECH.

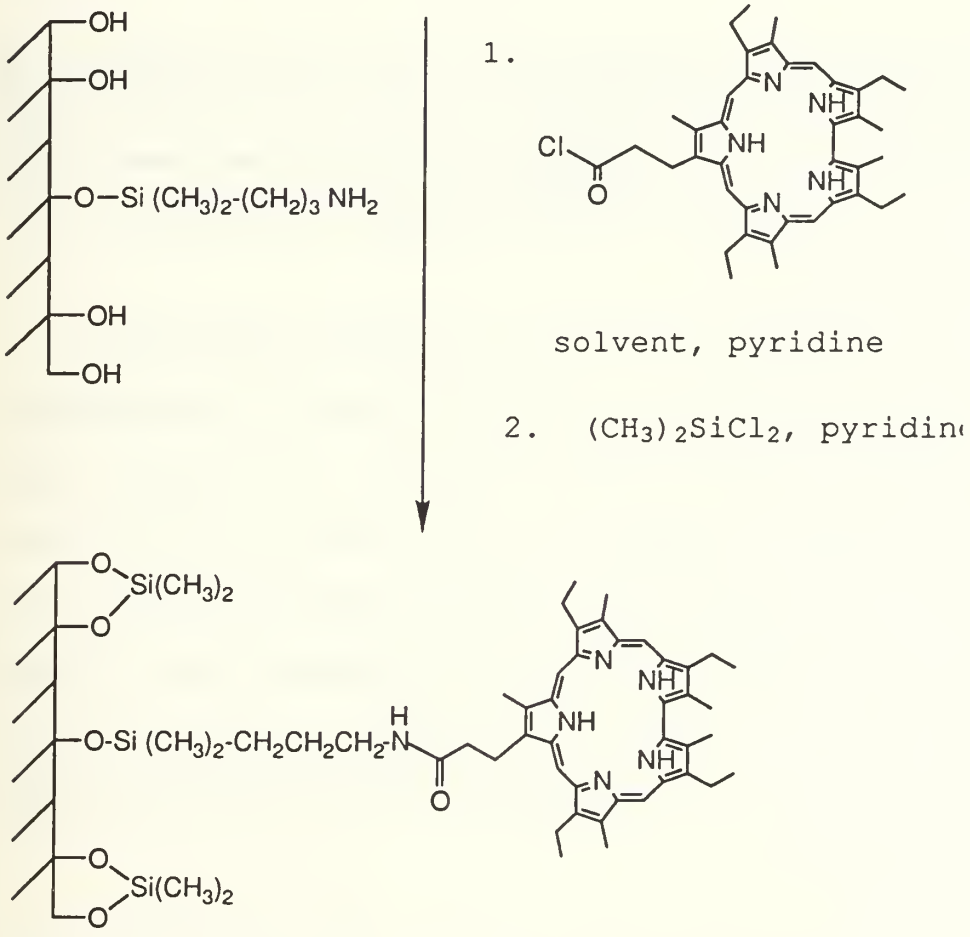


**Figure 19.** Synthesis of sapphyrin-modified silica gel.

**Effect of PH Variation on AMP Retention on SG-1.** Under isochratic HPLC conditions of 0.2 mL/Min flow, using 100 mM ammonium phosphate (dibasic), the pH of the buffer was varied to investigate the effect on retention of 5'-AMP on the 4.6 mm x 10 cm SG-1 column. The pH was varied from 5.6 to 8.0. In this pH range, the sapphyrin is monoprotonated. The results are shown in table 12. The results showed the shortest retention time for AMP to be at pH 7.0.

| pH of Buffer | Retention Time (minutes) |
|---|---|
| 5.6 | 40.6 |
| 7.0 | 23.2 |
| 8.0 | 24.5 |

**Table 12.** Retention times for 5'-AMP at varying pH.

**Nucleotide Retention on SG-1.** The retention of various monophosphates, as well as the mono- to triphosphates of adenosine were checked at pH 7.0 on the SG-1 column. Isochratic HPLC conditions of 0.10 mL/min and 100 mM ammonium phosphate were used. The results are shown in Table 13. The results clearly show the retention time increases with the number of phosphates present. The results also show a remarkable preference for the 5'-adenosine monophosphate over the other monophosphates

| COMPOUND | Retention Separately (min) | Retention of Aden Series Mix (min) |
|---|---|---|
| Adenosine | 23.2 | 23.2 (11.4)* |
| 5'-AMP | 45.8 | 45.8 (21.4)* |
| 5'-CMP | 23.7 | |
| 5'-GMP | 29 | |
| 5'-UMP | 25.7 | |
| 5'-ADP | 112.4 | 112.4(44.4)* |
| 5'-ATP | 150.1 | 150.9 (105.5)* |

**Table 13.** Retention times for nucleotides. *Indicates run at 0.20 mL/min.

**Retention of Polydeoxyadenylic Acids on SG-1.** The 3- through 5-mers of polydeoxyadenylic acid were checked for variations in retention time versus the number of phosphates. Isochratic HPLC conditions of 0.20 mL/min flow and 100 mM ammonium phosphate were used. The results are shown in Table 14.

| | Retention Time (min) 0.20 mL/min | Retention Time (min) 0.35 mL/min |
|---|---|---|
| $p(dA)_3$ | 100.0 | 32.0 |
| $p(dA)_4$ | 220.0 | 63.7 |
| $p(dA)_5$ | 460.0 | 123.0 |
| $p(dA)_6$ | 820.0 | 289.0 |

**Table 14.** Retention times of the $p(dA)_{3-6}$ series.

**Retention Times of Various Anions on SG-2 and Control Column.** Various anions were injected onto SG-2 under

isochratic conditions of 0.2 mL/min and 100 mM ammonium phosphate. The anions were also injected onto the control column under under the same isochratic conditions to check for retention times. The results are shown in Table 15.

| Solution | $pk_1$ | $pk_2$ | pH | Charge | Retention Time Control Column (min) | Retention Time Sapphyrin Column (min) |
|---|---|---|---|---|---|---|
| Benzophenone | | | 6 | | 6.8 | 6.4 |
| Benzenesulfonic Acid | 2.55 | | 6 | -1 | 5.9 | 8.3 |
| Benzoic Acid | 4.20 | | 6 | -1 | 5.0 | 10.4 |
| Phenylphosphinic Acid | 2.10 | | 6 | -1 | 5.8 | 10.7 |
| Phenylphosphonic Acid | 1.83 | 7.07 | 6 | -1 | 5.9 | 12.0 |
| Phenylacetic Acid | 4.31 | | 6 | -1 | 5.7 | 12.9 |
| Diphenylacetic Acid | 3.94 | | 6 | -1 | 8.2 | 14.3 |
| Phenylarsonic Acid | 4.53 | 9.52 | 6 | -1 | 6.1 | 16.0 |
| Diphenylphosphoric Acid | 1.85 | | 6 | -1 | 5.9 | 20.5 |
| Homopthalic Acid | 2.95 | 5.41 | 7 | -2 | 5.7 | 9.9 |
| Benzylphosphonic Acid | 2.38 | 5.98 | 7 | -2 | 6.0 | 14.6 |
| Phenylphosphoric Acid | 1.48 | 5.70 | 7 | -2 | 5.6 | 15.3 |

**Table 15.** Retention times for various anions ($\pm$0.2 min).

**Retention Times for Nucleotides on SG-2.** The adenosine series of nucleotides were injected under various isochratic conditions of 0.20 to 1.0 mL/min and 0.5 to 1.0 mM ammonium phosphate were used to check retention times. The results are shown in Table 16.

| | Retention Time (min) 1 M & 0.5 mL/min | Retention Time (min) 1 M & 0.2 mL/min | Retention Time (min) 0.5 M & 1 mL/min | Retention Time (min) 0.5 M & 0.8 mL/min |
|---|---|---|---|---|
| Adenosine | 2.6 | 7.5 | 1.3 | 1.7 |
| 5′-AMP | 5.0 | 12.5 | 2.7 | 3.4 |
| 5′-ADP | 6.3 | 14.8 | 3.9 | 4.9 |
| 5′-ATP | 7.5 | 17.5 | 5.6 | 6.9 |

**Table 16.** Retention times of the adenosine series on SG-2.

**Retention Times of $P(dA)_{2-9}$ on SG-2.** The retention times of the $p(dA)_{2-9}$ series were determined under isochratic HPLC conditions of 1.0 mL/min and 1.0 M ammonium phospahte. It was found that the retention time increased with the number of phosphates present.

| | Retention time (min) |
|---|---|
| $p(dA)_2$ | 2.4 |
| $p(dA)_3$ | 3.7 |
| $p(dA)_4$ | 5.1 |
| $p(dA)_5$ | 7.3 |
| $p(dA)_6$ | 10.6 |
| $p(dA)_7$ | 15.2 |
| $p(dA)_8$ | 21.1 |
| $p(dA)_9$ | 30.7 |

**Table 17.** Retention times of p(dA)2-9. Average of 2 runs, error of $\pm$ 0.2 min.

**Retention Times of P(dC)-p(dA) Mixes on SG-2.** The p(dC)-p(dA) retention times were determined under isochratic HPLC conditions of 0.10 mL/min of 0.5 M ammonium phosphate. It was determined that a mix could be separated. The results are shown in Table 18.

| | Retention Time (min) $p(dA)_3$, $p(dA)_4$, $p(dA)_5$, $p(dA)_6$ | Retention Time (min) $p(dC)_3$, $p(dA)_4$, $p(dC)_5$, $p(dA)_6$ |
|---|---|---|
| $p(dA)_3$ or $p(dC)_3$ | 27.6 | 20.2 |
| $p(dA)_4$ | 38.0 | 36.6 |
| $p(dA)_5$ or $p(dC)_5$ | 51.3 | 46.5 |
| $p(dA)_6$ | 76.7 | 77.2 |

**Table 18.** Retention times of p(dA)-p(dA) mixes.

**Retention Times on DEAE Columns.** The various anionic species injected on the sapphyrin-silica gels were injected onto a commercial DEAE column at neutral pH to check for anion selectivity. Isochratic HPLC conditions of 0.4 mL/min and 0.5 mM ammonium phosphate were used. The results are shown in Table 19.

| Solution | Retention Time (min) Control Column |
|---|---|
| Benzophenone | 23.4 |
| Benzenesulfonic Acid | 8.8 |
| Benzoic Acid | 10.4 |
| Phenylphosphinic Acid | 5.8 |
| Phenylphosphonic Acid | 5.9 |
| Phenylacetic Acid | 5.7 |
| Diphenylacetic Acid | 8.2 |
| Phenylarsonic Acid | 6.1 |
| Diphenylphosphoric Acid | 5.9 |
| Homopthalic Acid | 5.7 |
| Benzylphosphonic Acid | 6.0 |
| Phenylphosphoric Acid | 5.6 |

**Table 19.** Anion retention times on DEAE column.

**Column Efficiency of SG-2.** The column efficiency, or number of theoretical plates, was determined by eluting benzene under isochratic conditions of methanol/water (50/50) and 0.1 mL/min flow. The efficiency was determined from the average of four runs. The results are given in Table 20.

| Run | $t_r$(min) | $t_w$(min) | N |
|---|---|---|---|
| 1 | 7.4 | 1.6 | 327 |
| 2 | 8.1 | 1.2 | 846 |
| 3 | 7.9 | 1.2 | 628 |
| 4 | 8.1 | 1.4 | 535 |
| Average | 7.9 | 1.4 | 584 |

**Table 20.** Determination of column efficiency.

**Stationary Phase Coverage.** The stationary phase coverage was determined by the method of Unger (156). It relies on the elemental analysis of the silica gels. The results are shown in Table 21.

| Silica | Surface Area ($m^2$/mg) | %C | %N | Coverage (mmol/$m^2$) |
|---|---|---|---|---|
| Amino-propyl | 480 | 4.85 | 1.62 | 2.58 |
| Silyl-ated | 480 | 5.57 | 1.45 | 0.66 |
| **SG-2** | 480 | 7.32 | 1.85 | 0.124 |

**Table 21.** Stationary phase coverage.

**Energetics of Binding.** The change in Gibbs Free Energy per phosphate can be determined by the method outlined in the Methods section. The graphs of retention time versus number of phosphates and change in free energy per phosphate are shown in Figures 20-23 as well as representative HPLC chromatographs. The results are shown below for the $p(dA)_{2-9}$ case.

Plotting the change in free energy versus the number of phosphates shows free energy values of 233, 200, and 270 cal/mol per phosphate for the p(dA), p(dC), and adenosine phosphate series respectively.

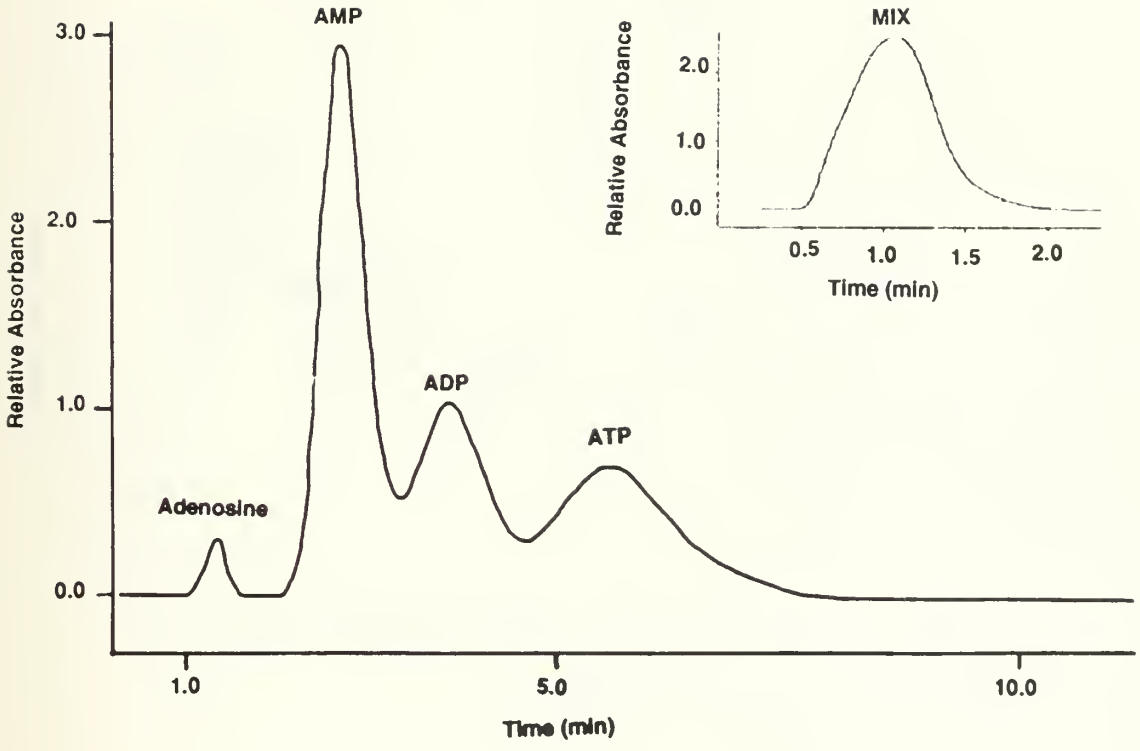


**Figure 20.** Chromatogram of p(dA)2-9 separation under isochratic conditions.

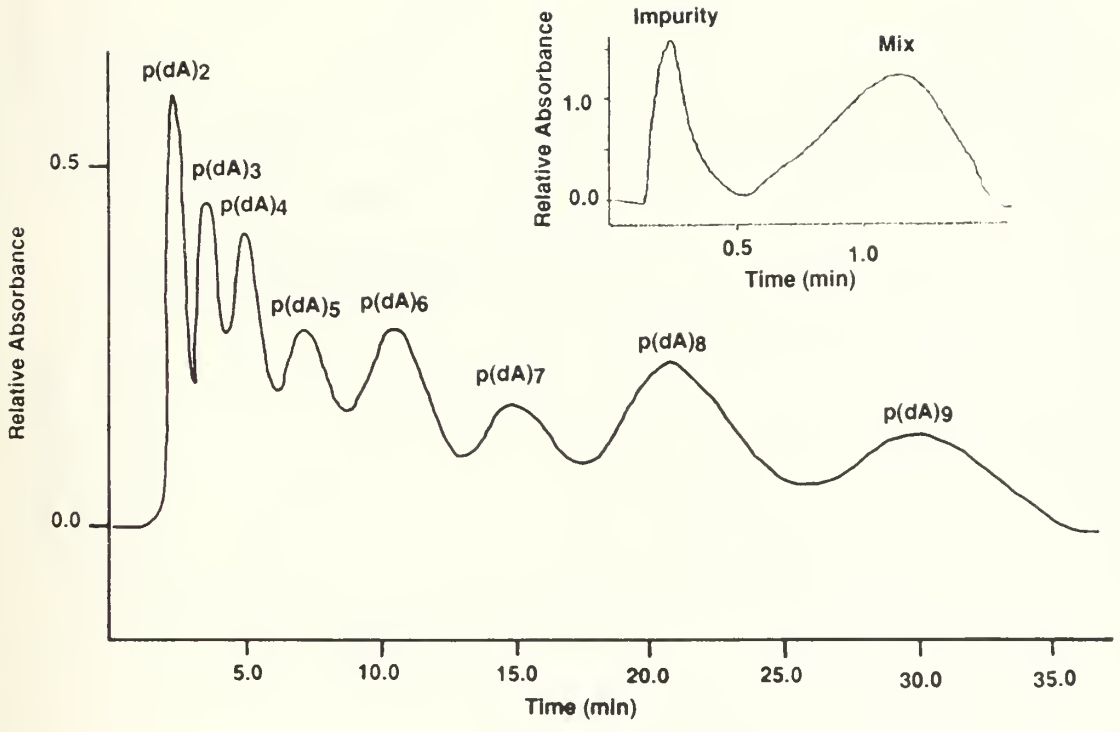


**Figure 21.** Chromatogram of adenosine, AMP, ADP, and ATP separation under isochratic conditions.

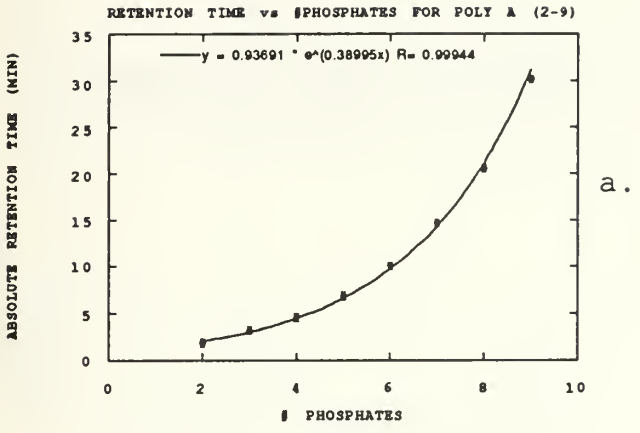


a.

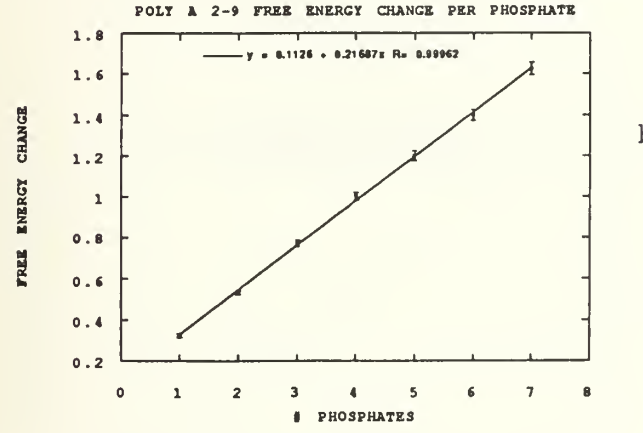


b.

**Figure 22.** Changes in retention times (a.), and free energy (b.), per phosphate for the p(dA)2-9 series.

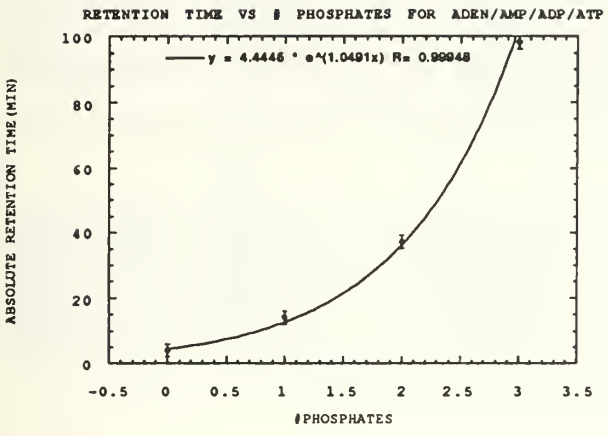


c.

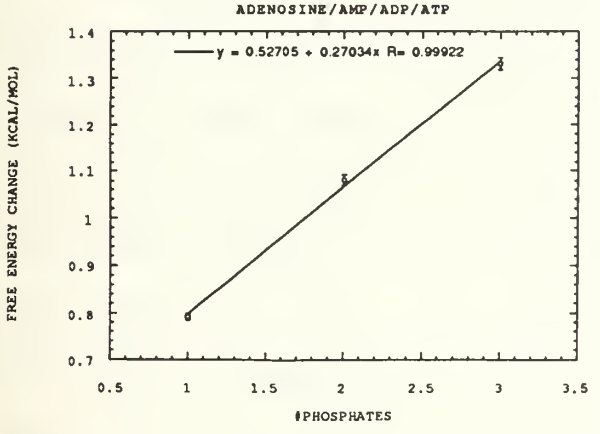


d.

**Figure 23**. Changes in retention times (a.), and free energy (b.), per phosphate for the adenylate series.

| #Phosphates | $t_r-t_o$ (min) | k′ | $a=k_x/k_{x+1}$ | $\Delta\Delta G°$/ phosphate (cal/ mol) |
|---|---|---|---|---|
| 2 | 0.7 | 0.412 | | |
| 3 | 2.1 | 1.235 | 0.334 | |
| 4 | 3.4 | 2.000 | 0.6195 | 284.9 |
| 5 | 5.7 | 3.350 | 0.597 | 304.5 |
| 6 | 8.8 | 5.180 | 0.647 | 257.3 |
| 7 | 13.5 | 8.06 | 0.643 | 261.1 |
| 8 | 19.5 | 11.47 | 0.703 | 208.0 |
| 9 | 29.3 | 17.24 | 0.665 | 240.5 |

**Table 22.** Free energy per phosphate for the p(dA) series.

| | $t_r-t_o$ | k′ | $a=k_x/k_{x+1}$ | $\Delta\Delta G°$/ phosphate (cal/ mol) |
|---|---|---|---|---|
| Adenosine | 0.6 | 0.35 | | |
| AMP | 2.4 | 1.42 | 0.25 | 818 |
| ADP | 3.8 | 2.23 | 0.63 | 272 |
| ATP | 5.8 | 3.41 | 0.654 | 251 |

**Table 23.** Free energy per phosphate for adenosine series.

**Sapphyrin Dimer-EDTA Conjugate.** The sapphyrin dimer EDTA conjugate was synthesized several times by the method shown in figure 24. The synthesis consisted of a modular construction of the molecule using a series of amide couplings. The major problem associated with this molecule is solubility, of rather a lack of solubility in solvents. The sapphyrin dimer and the sapphyrin dimer-EDTA conjugate could not be characterized by proton NMR in any of a variety of deuterated solvents. Proton NMRs were attempted in deuterated versions of chloroform, dichloromethane, dimethylsulfoxide, methanol, benzene, and pyridine. These NMRs could not be interpreted due to problems with solubility and aggregation. The sapphyrin dimer-EDTA conjugate also proved to be difficult to deprotect.

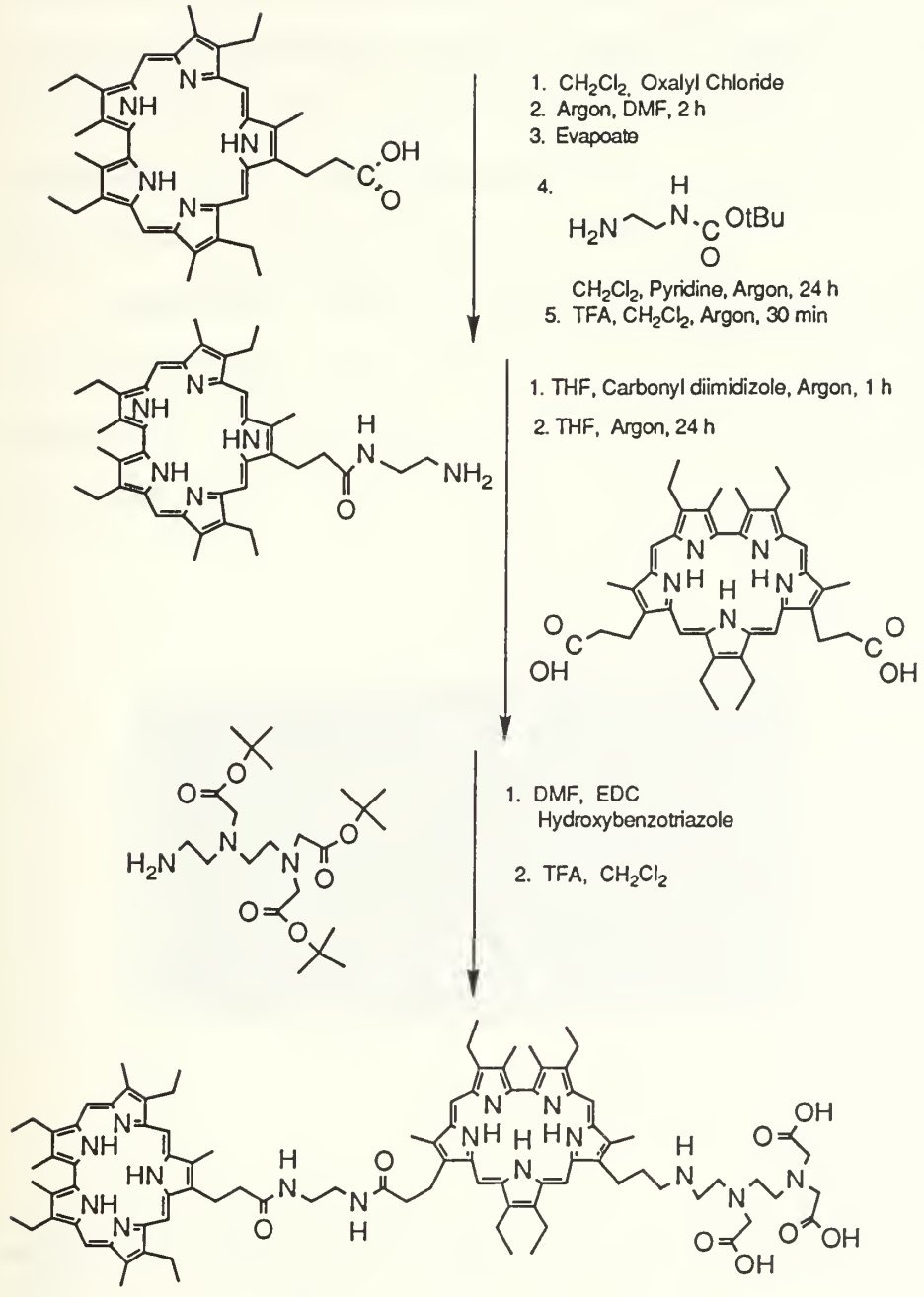


**Figure 24.** Synthesis of sapphyrin dimer-EDTA conjugate.

Several attempts were made to deprotect. Deprotection was finally accomplished, but the conjugate proved difficult to characterize. The sapphyrin dimer-EDTA conjugate seemed to readily complex copper from the mass spectra probe. It was shown by low resolution mass spectra that an iron molecule could be complexed, but high resolution mass spectra could not be obtained.

**Supercoiled Assay**. Figure 25 shows the results of the supercoiled assay. The sapphyrin dimer-EDTA conjugate did not appear to show any higher activity than Fe-EDTA at the same concentration.

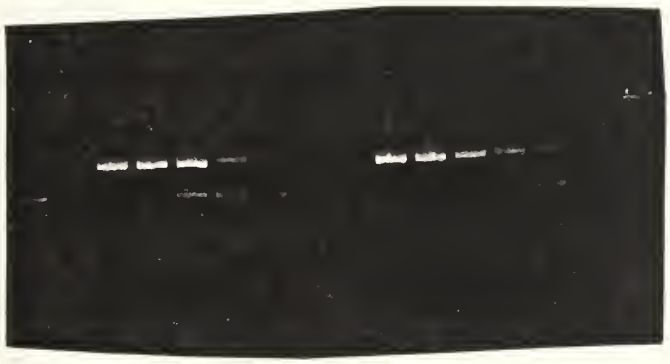

**Figure 25**. Supercoiled assay. Each lane contains 7 µL of pipes (5 mM), 0.6 µL ofsupercoiled DNA, and 1 µL of DTT (10mM). Lanes in order of left to right, 1. DNA only, 2. 10 µM sapphyrin dimer, 3. 5 µM dimer, 4. 2.5 µM dimer, 5. 1.25 µM dimer, 6. 0.67 µM dimer, 7. 10 µM FeEDTA, 8. 5 µM FeEDTA, 9. 2.5 µM FeEDTA, 10. 1.25 µM FeEDTA, 11. 0.67 µM FeEDTA. The bands are from top to bottom, nicked supercoiled DNA, and supercoiled.

**Calf Thymus DNA Titration.** The titration of 6 mM of the sapphyrin dimer-EDTA conjugate showed no spectral shifts. The absorption spectra indicated that the conjugate was in a state of aggregation, even with 10% Tween or SDS. As, calf thymus DNA was titrated in there was no significant change in the spectra. The amount of calf thymus added was from 1 to 100 equivalents of DNA phosphates. The sapphyrin monomer-EDTA conjugate showed an 11nm bathochromic shift of its singular Soret band. The results seen for the dimer are shown in table 24. These results indicate there was no binding interaction seen between the dimer conjugate and the calf thymus DNA.

| DNA EQUIV PHOSPHATES | 424.4 nm Soret [Abs] | 450.4 nm Soret [Abs] |
|---|---|---|
| 0 | 0.120 | 0.144 |
| 1 | 0.114 | 0.138 |
| 10 | 0.112 | 0.137 |
| 50 | 0.124 | 0.132 |
| 100 | 0.108 | 0.129 |

**Table 24.** Titration of sapphyrin dimer-EDTA conjugate with calf thymus DNA.

## B: Discussion

**Sapphyrin-Modified Silica Gel.** The sapphyrin-modified silica gel shows selectivity for certain anionic species under isochratic HPLC conditions. The results do not appear to represent a purely π-stacking or hydrophobic event. The benzophenone or benzene species, which are neutral, are not retained to any great extent. We however see that various monoanionic and polyanionic species are retained to differing extents. These results can be compared with those seen in the case of the DEAE column. The DEAE column does interact with anions through some hydrophobic weak anion exchange principles. We can see a marked difference in the order of retentions under neutral, isochratic HPLC conditions.

There is also strong evidence that the interaction seen is not the result of pure electrostatics. There is a wide range of retention times for monoanionic species. For example, benzenesulfonic acid is retained for 8.3 minutes, while diphenylphosphoric acid is retained for 20.5 minutes under the same conditions. The homopthalic acid, which is dianionic, is retained for only 9.9 minutes. Thus, the results seen cannot be a totally electrostatic phenomenon. The interaction appears to be the result of the phosphate chelation interaction proposed.

There appears to be a correlation between the accessibility of the oxyanion and the anion selectivity. The central atom-to-oxygen distances for benzenesulfonate, phenylphosphonate, and phenylarsonate are 1.47, 1.52, and 1.69 Å respectively (155). If we accept the idea of phosphate chelation being the mode of interaction, we would predict that longer central atom-to-oxygen bonds would result in longer retention times. This is exactly what is seen.

The fact that oligonucleotides are retained according to the number of phosphates present is expected. In calculating the free energy change per phosphate we see that the effect of each additional phosphate group is additive. This again is consistent with phosphate chelation.

**Sapphyrin Dimer-EDTA Conjugate.** The sapphyrin dimer-EDTA conjugate proved difficult to characterize. It appeared to be aggregated under aqueous conditions. Combined with the low solubility, this is presumed to have prevented the conjugate from binding to the DNA phosphates. This sapphyrin dimer-EDTA conjugate was not pursued further due to the lack of activity with supercoiled DNA and calf thymus DNA.

It is possible to imagine improving the solubility of sapphyrin dimers by adding water solubilizing molecules such as sugars. There is also the possibility of using a more rigid linker to prevent the intramolecular interaction from preventing

interaction with DNA phosphates. The most probable success would come from incorporating both a water solubilizing group and a more rigid linker.

## B: Conclusions

**Sapphyrin-modified Silica Gels.** The sapphyrin-modified silica gels provide a valuable insight into the anion selectivity of sapphyrin. The nature of the this sapphyrin-anion interaction appears to be based on the accessibility of the oxyanion for chelation to the basic sapphyrin core. This allows us to accurately predict the selectivity of sapphyrin for various anions in solution.

The sapphyrin-silica gels also proved to be capable of efficient separation of oligonucleotides and nucleotides. Thus, the process of attaching macrocycles to solid supports can be expanded to studying the binding properties of other expanded porphyrin macrocycles. One sees that in probing the interaction of receptor-substrate interactions, feasible applications of these receptor-modified supports may be realized.

**Sapphyrin-Dimer.** The sapphyrin dimer-EDTA conjugate proved to be ineffective in interacting with DNA. The fact that this molecule does not interact with DNA led us to discontinue work with this particular molecule. There are several other people in this group who are synthesizing sapphyrin dimers with different linkers and water solubilizing groups.

## B: Experimental

**Materials and Methods.** Solvents and reagents were purchased commercially. They were of reagent quality and used without further purification, unless otherwise noted.

$^{1}H$ and $^{13}C$ NMR spectra were measured on a Bruker AC 250 MHz instrument or GE 300Mhz instrument and are reported in parts per million (ppm) of tetramethylsilane. Elemental analyses were performed by Atlantic Microlab, Inc. Fast atom bombardment (FAB) mass spectra were performed by the University of Texas Mass Spectral Facility at Austin, Texas.

Low pressure liquid chromatography was performed using a PrepRPC 15 mM reverse phase column using a Pharmacia LKB fast protein liquid chromatograph (FPLC), with 2 P-500 pumps, a GP-250 controller, and UV-2 dual path monitor. Analytical HPLC was performed using either a Hewlett-Packard 1090M liquid chromatograph with a 8452A diode array detector, or a Varian LC Star 9002 Solvent Delivery System with a Varian LC Star 9050 UV-Vis Detector.

The aminopropyl silica gel (Aldrich) used to prepare the sapphyrin-silica gel columns consisted of spherical particles with a mean diameter of 52 mm, a pore diameter of 60 Å, a pore volume of 0.75 $cm^3/kg$, and a surface area of 480 $m^2/g$. HPLC analytical columns were custom packed by Alltech Chromatography into 4.6 mm x 10 cm columns.

**Effect of Varying pH on Retention of AMP on Column SG-1.** Adenosine 5′-monophosphate (5 mM) was injected onto the Hewlett Packard HPLC in 10ml amounts. The pH of the buffer (100 mM $(NH_4)_2HPO_4$) was adjusted to 5.6, 7.0, and 8.0. Isochratic HPLC conditions with a flow of 0.2 mL/min were used. Differences in retention times were determined by monitoring 260 nm.

**Determination of Retention Times for Nucleotides on SG-1.** Solutions of 5′-AMP, 5′-CMP, 5′-GMP, and 5′-UMP (5 mM) were prepared. The solutions were injected (20 mL) singularly and in mixtures. Isochratic HPLC conditions of 0.10 mL/min of 100 mM $(NH_4)_2HPO_4$ were used. Data was recorded at 260 nm. The mono- to tri-phosphates of adenosine were repeated at 0.20 mL/min.

**Determination of Retention Times for Polydeoxyadenylic Acid [p(dA)]on SG-1.** Solutions of $p(dA)_{3-6}$ were prepared as follows. Five units of the p(dA) were dissolved in pipes buffer (5 mM, pH 7.0). The solutions were injected (20 mL) as a mixture. Isochratic HPLC conditions of 0.20 mL/min of 100 mM $(NH_4)_2HPO_4$ and pH 7.0 were used. Data was recorded at 260 nm. The run was repeated at 0.35 mL/min.

**Determination of Retention Times for Various Anions on SG-1.** Solutions of various anions in $H_20$ were prepared. For each anion, 15 mL were injected under isochratic conditions with $(NH_4)_2HPO_4$ (100mM) at pH 6.0 or pH 7.0 and a flow rate of 0.2 mL/min. Runs were monitored at 210 and 260 nm.

**Retention Times on Control Column.** The previous procedures were repeated using the silyl-capped control column (no sapphyrin).

**Determination of Retention Times for Nucleotides on SG-2.** Solutions of adenosine, 5′-AMP, 5′-ADP, and 5′-ATP (5 mM) were prepared. The solutions were injected (20 mL) as a mixture. Isochratic HPLC conditions of 0.20 to 1.0 mL/min of 0.5 to 1.0 mM $(NH_4)_2HPO_4$ were used. Data was recorded at 260 nm.

**Determination of Retention Times for Polydeoxyadenylic Acid [p(dA)]on SG-2.** Solutions of $p(dA)_{2-9}$ were prepared as follows. 5 units of the p(dA) were dissolved in pipes buffer (5 mM, pH 7.0). The solutions were injected (20 mL) as a mixture. Isochratic HPLC conditions of 1.0 mL/min of 1.0 M $(NH_4)_2HPO_4$ and pH 7.0 were used. Data was recorded at 260 nm.

**Determination of Retention Times for Polydeoxycytidilic Acid [p(dC)]on SG-2.** Solutions of $p(dC)_{3-5}$ were prepared as follows. Five units of the p(dC) were dissolved in pipes buffer (5 mM, pH 7.0). The solutions were injected (20 mL) as a mixture. Isochratic HPLC conditions of 0.10 mL/min of 500 mM $(NH_4)_2HPO_4$ and pH 7.0 were used. Data was recorded at 260 nm.

**Retention Times of Anionic Species on DEAE Column.** Various anionic species were injected onto the DEAE column (Rainin). They were injected under isochratic condition of 0.5 M

$(NH_4)_2HPO_4$ at 0.4 mL/min. Retention times were monitored at 210 or 260 nm.

**Determination of Column Efficiency of SG-2.** A solution of benzene (5 mM) was injected (15 mL) under isochratic conditions of MeOH/$H_2O$ (50:50) and 0.1mL/min. Column efficiency, or the number of theoretical plates is calculated by:

$$N = 16(t_r / t_w)^2$$

Where, $t_r$ is the retention time for benzene, and $t_w$ is baseline peak width.

**Determination of Stationary Phase Coverage.** The surface concentration of the sapphyrin on the stationary phase is calculated by (156):

$$\text{Coverage} = (\%X \times 10^6) / \{(AM)n100[1-\%X(MW)/(AM)n100]S\}$$

Where %X is the percentage increase in carbon or nitrogen as determined by elemental analysis. AM is the atomic mass of carbon or nitrogen. MW is the molecular weight of the bound species. *n* is the number of carbon or nitrogen in the bound species. S is the surface area of the silica gel in $m^2/gm$.

**Calculation of Energetics.** Retention time versus number of phosphates was plotted for the p(dA), p(dC), and monoadenosine phosphate series. Retention times were normalized by calculating capacity factors (157):

$$k' = (t_r - t_o)/t_o$$

The selectivity , $\alpha$ (158), for one anion over the other:

$$\alpha = k'_1/k'_2$$

The capacity factor is also related to the equilibrium distribution, K:

$$k' = K\Phi$$

Where $\Phi$ is the phase ratio, or ratio of volumes between the stationary and mobile phases. As K is the ratio of the number of moles of the solute in the stationary phase and mobile phase, we can relate K and the Gibbs Free Energy, $\Delta G^\circ$:

$$K = e^{\Delta Go/RT}$$

Thus, for different peaks we can find the Gibbs Free Energy difference, $\Delta\Delta G^\circ$:

$$k'_1/k'_2 = (e^{\Delta G_1 o/RT})/(e^{\Delta G_2 o/RT})$$

This can be reduced to:

$$\ln \alpha = e^{-\Delta\Delta Go/RT}$$

We then plot $\Delta\Delta G^\circ$ versus the number of phosphates. From the resulting straight lines, we can determine free energy per phosphate.

**N-(t-butylcarbonyl)-diaminoethane.** Di-tert-butyl-dicarbonate (17.9 mg, 79 mmol) was dissolved in chloroform (200 mL). Ethylene diamine (30.0mL, 449 mmol) was added dropwise. The mixture was stirred at room temperature for 19 h. The solvents were rotary evaporated. The residue was extracted with sodium carbonate (100 mL) and dichloromethane (100mL). The aqueous layer was washed

with dichloromethane (100 ml). The dichloromethane layers were combined and evaporated. The yellow oil was subject to column chromatography with $CH_2Cl_2$/methanol (90%:10%). The fraction containing the protected amine was evaporated and yielded 10.7mg (83%) of the product. 1H NMR ($CDCl_3$) δ 1.44 (9H,s,$CH_3$), 1.604 (2H,br,$CH_2$), 2.8 (2H, m, $CH_2$), 3.189 (2H, m, $NH_2$), 4.893 (1H, br, NH). $^{13}C$ NMR ($CDCl_3$) δ 28.41, 41.834, 43.315, 79.263, 156.21. LRMS: 161.1 (Calculated for $C_7H_{17}N_2O_2$ : 161.200).

**3,8,17,22-Tetraethyl-12-(N-t-butylcarbonyldiamidoethyl)-2,7,13,18,23-pentamethyl-sapphyrin**. Sapphyrin mono-acid (39 mg, 0.062 mmoL) was dissolved in dry dichloromethane (15 mL). Oxalyl chloride (0.3 mL, 0.6 mmol) and 4 drops DMF were added. The reaction was stirred under Argon for 2 h. The solvents were removed *in vacuo*. The residue was dissolved in dry dichloromethane (10 mL). Protected amine (32 mg, 0.2 mmol) in dry dichloromethane (10 mL) and pyridine (0.1 mL) was slowly added by dropping funnel. The mixture was stirred overnight under Argon. The solvents were removed by rotary evaporation. The resulting oily substance was washed with ddH2O and sodium bicarbonate. After evaporation the product was dissolved in dichloromethane and purified by column chromatography with dichloromethane/MeOH (99:1). The dark fraction was evaporated to give 40 mg (86%) of the protected sapphyrin-amide. 1H NMR: ($CDCl_3$) δ -5.05 (2H, m, *NH*), -4.75 (3H, br-m, *NH*), 1.5 (9H, s, $CO_2(CH_3)_3$),

2.3 (6H, t, $CH_2CH_3$), 2.5 (3H, t, $CH_2CH_3$), 2.74 (3H, t, $CH_2CH_3$), 3.5 (4H, $NHCH_2CH_2$), 4.3 (6H, s, $CH_3$), 4.35 (6H, s, $CH_3$), 4.45 (3H, s, $CH_3$), 4.7 (8H, q, $CH_2CH_3$), 5.0 (4H, m, $CH_2CH_2CONH$), 7.4 (2H, s, CONH) 11.5 (1H, s, meso-H), 11.75 (3H, s, meso-H) FAB MS m/e (rel. intensity) 771 (28, [M-1]), 772 (100, [M]), 773 (59,[M+1]), 774 (16, [M+2]). $^{13}C$ NMR ($CDCl_3$) ..... HRMS: 772.4914 (Calculated for $C_{47}H_{62}N_7O_3$: 772.4912).

**Sapphyrin Dimer.** The protected sapphyrin-amide (25 mg, 0.032 mmol) was dissolved in dry dichloromethane (1.5 mL) and trifluoroacetic acid (1.5 mL). The mixture was stirred under Argon for 30 min. The mixture was dried *in vacuo*. To the same flask was added solid sapphyrin di-acid (30 mg, 0.043 mmol), 1-ethyl-3-(3-dimethylaminopropyl carbodiimide hydrochloride (9 mg, 0.46 mmol), and hydroxybenzotriazole (6.4 mg, 0.42 mmol). A stir bar was added and the reaction vessel evacuated and flushed with Argon. Dry DMF (2 mL) was added by syringe and the reaction mixed overnight at room temperature. Dry dichloromethane (50 mL) was added and the solution washed with brine (3x), and then $ddH_2O$ (3x). The solvent was removed by rotary evaporation. The product was purified by column chromatography. The fraction collected was evaporated and yielded 35 mg (60 %) of the sapphyrin dimer. $^1H$ NMR ($CDCl_3$, $C_5D_5N$, $C_6D_6$, $CD_3OD$, $CD_3SOCD_3$, $CD_2Cl_2$)..... HRMS: 1346.846 (Calculated for $C_{84}H_{106}N_{12}O_4$: 1346.838).

**Sapphyrin Dimer-EDTA Conjugate**. The tritylated EDTA ligand (300 mg, 0.43 mmol) was dissolved in dry methanol (10 ml). Pearlman's Pd catalyst (200 mg) was added. The reaction was covered and stirred under Argon for 18 h. The mixture was filtered through a medium frit and washed with chloroform. The product was purified by column chromatography with $CH_2Cl_2$/MeOH (85:15). Solvents were removed by rotary evaporation. The EDTA ligand (5 mg, 0.011 mmol), sapphyrin dimer (8 mg, 0.0059 mmol), EDC (2.5 mg, 0.012 mmol), and HOBT (2.0 mg, 0.013 mmol) were placed in a flask. The flask was evacuated and flushed with Argon. Dry DMF (2.0 ml) was added by syringe. The reaction was stirred 20 h at room temperature. Dry $CH_2Cl_2$ (50 ml) was added, and the mixture washed with brine (3x) and $ddH_2O$ (3x). The product was purified by column chromatography. After rotary evaporation 6 mg (58 %) of the protected sapphyrin-dimer-EDTA conjugate were obtained. . $^1H$ NMR ($CDCl_3$, $C_5D_5N$, $C_6D_6$, $CD_3OD$, $CD_3SOCD_3$, $CD_2Cl_2$)..... FAB MS m/e (rel. intensity) 1767 (24, [M-3]), 1768 (45, [M-2]), 1769 (80, [M-1]), 1770 (100,[M]), 1771 (93, [M+1]), 1772 (51, [M+2]), 1773 (28, [M+3]). Vis $\lambda_{max}$ ($CHCl_3$) (Abs)= 454 (2.39), 624 (0.11), 676 (0.12), 686(sh) (0.12). HRMS: 1769.111 (Calculated for $C_{106}H_{142}N_{15}O_9$: 1769.16).

The protected conjugate (5 mg, 0.0028 mmol) was dissolved in TFA (2 mL) and allowed to stand for 1 hour. The solution was evaporated, and then washed with $CH_2Cl_2$ (3x) and MeOH(3x). After rotary evaporation 4.0 mg of the deprotected complex was obtained. $^1H$ NMR

($CDCl_3$, $C_5D_5N$, $C_6D_6$, $CD_3OD$, $CD_3SOCD_3$, $CD_2Cl_2$)..... Vis $\lambda_{max}$ (MeOH/$CHCl_3$, 10:90) (Abs)= 454 (2.24), 622 (0.14), 676 (0.13), 686(sh) (0.13). Vis $\lambda_{max}$ (5mM Pipes) (Abs)= 454 (0.33), 424 (sh)(0.15), 612 (0.1), 670 (0.1). Vis $\lambda_{max}$ (5mM Pipes, 10% Tween) (Abs)= 454 (0.13), 424 (0.1). FAB MS m/e 1601 (13.51, [M-1]), 1602 (17.45, [M]), 1603 (15.43, [M+1]), 1604 (14.62, [M+2]), 1605 (14.28, [M+3]), also on several others 1665 ([M+63(Cu)]), and one 1657 ([M+57(Fe)).

**Supercoiled DNA Assay**: A stock solution of the sapphyrin-dimer EDTA conjugate (SDE) (1 mM) was prepared in $H_20$ with 10 % Tween for solubility. A solution of Fe (II)-SDE was prepared by adding $Fe(NH_4)_2SO_4$ (25 mM, 200 mL) to SDE (50 mM, 200 mL). A solution of Fe(II)-EDTA was prepared by adding $Fe(NH_4)_2SO_4$ (25 mM, 200 mL) to EDTA (50 mM, 200 mL). Reactions were set-up in Eppendorf tubes. To each tube was added pipes buffer (7 mL, 5 mM), dithiothreitol (DTT) (1 mL of 20 mM), supercoiled DNA, pBR322, (1 mL of 0.357 mg/mL), and either SDE or EDTA complexed with Fe(II). The concentrations of the Fe(II) complexes were 25, 12.5, 6.25, 3.12, and 1.61 mM. One tube contained pipes buffer (8 mL, 5 mM), dithiothreitol (DTT) (1 mL of 20 mM), supercoiled DNA, pBR322, (1 mL of 0.357 mg/mL). The reaction stopped with bromophenol blue (2 mL) after 30 minutes. The reactions were loaded onto a agarose gel (1 % in TAE) containing ethidium bromide (6 mL). The gel was run at 80 volts. The results were visualized under a UV lamp.

**Titration of SDE with Calf Thymus DNA.** A solution of calf thymus DNA (1 mg/mL) was prepared in pipes buffer (1 mM), this is equivalent to ~3 mM DNA phosphates. A solution of SDE (3 mM) was prepared in pipes buffer with 10 % Tween for solubility. The SDE solution was placed in a cuvette (1 mL). DNA was added from 1 to 200 DNA phosphate equivalents. The solution was monitored by UV-Vis.

## Bibliography


1. Voet, D.; Voet, J.G. in "Biochemistry," John Wiley & Sons, Inc., New York **1990**, 1095-1111.
2. Miller, K.L. in "Immunology: Clinical, Fundamental, and Therapeutic Aspects," ed. by Ram, B.P.; Harris,M.C.; Tyle,P., VCH Publishers, Inc., New York **1990**, 11-48.
3. Roitt, I.M. "Essential Immunology,4$^{th}$ ed.," Blackwell Scientific Publications, Oxford **1980**, 121-136.
4. Siskind, G.W.; Banceraf, B. in "Advances in Immunology, Vol. 10,"ed. by Dixon, F.J.; Kunkel, H.G., Academic Press, New York **1969**, 1-50.
5. Burnet, F.M. *Australian J. Sci.* **1957**, *20*, 67.
6. Burnet, F.M. "The Clonal Selection Theory of Immunity," Vanderbilt and Cambridge Univ. Presses, London **1959**.
7. Burnet, F.M. *Cold Spring Harbor Symp. Quant. Biol.* **1967**, *32*, 1.
8. Heidelberger, M; Kendall, F.E. *J. Exptl. Med.* **1935**, *61*, 563.
9. Heidelberger, M; Kendall, F.E. *J. Exptl. Med.* **1935**, *62*, 697.
10. Landsteiner, K.; Van der Scheer, *J. Exptl. Med.* **1936**, *63*, 325.
11. Boyd, W.C.; Bernard, H. *J. Immunol.* **1937**, *33*, 111.
12. Raffel, S.; Pait, C.F.; Terry, M.C. *J. Immunol.* **1940**, *39*, 317.

13. Landsteiner, K. "The Specificity of Serological Reactions," Thomas, Illinois,1936.

14. Karush, F. *J. Am. Chem. Soc.* **1956**, *78*, 5519.

15. Nisnoff, A.; Shaw, A.R.; Pressman, D. *J. Immunol.* **1958**, *80*, 417.

16. Pauling, L.; Pressman, D.; Grossberg, A. *J. Am. Chem. Soc.* **1944**, *66*, 784.

17. Eisen, H.N.; Siskind, G.W. *Biochemistry* **1964**, *3*, 996.36.

18. Heidelberger, M; Kendall, F.E. *J. Exptl. Med.* **1937**, *65*, 647.

19. Heidelberger, M; Kendall, F.E.; Mayer, M. *J. Exptl. Med.* **1940**, *71*, 271.

20. Raffel, S.; Terry, M.C. *J. Immunol.* **1940**, *39*, 337.

21. Raffel, S.; Terry, M.C. *J. Immunol.* **1940**, *39*, 349.

22. Jerne, N.K. *Acta. Pathol. Microbiol. Scand. Suppl.* **1951**, *87*.

23. Talmage, D.W.; Maurer, P.H. *J. Infect. Diseases* **1953**, *92*, 288.

24. Farr, R.S. *J. Infect. Diseases* **1958**, *103*, 239.

25. Fazekas de St. Groth, S. *Cold Spring Harbor Symp. Quant. Biol.* **1967**, *32*, 525.

26. Hooker, S.B.; Boyd, W.C. *Proc. Soc. Exptl. Biol. Med.* **1941**, *47*, 187.

27. Siskind, G.W.; Dunn, P.; Walker, J.G. *J. Exptl. Med.* **1968**, *127*, 55.

28. Goidl, E.A.; Paul, W.E.; Siskind, G.W.; Benacerraf, B. *J. Immonol.* **1968**, *100*, 371.

29. Little, J.R.; Eisen, H.N. *Biochemistry* **1966**, *5*, 3385.

30. Fujio, H.; Karush, F. *Biochemistry* **1966**, *5*, 1856.

31. Zimmering, P.F.; Lieberman, S.; Erlanger, B.F. *Biochemistry* **1967**, *6*, 154.

32. Klinman, N.R.; Rockey, J.H.; Frauenberger, G.; Karush, F. *J. Immunol.* **1966**, *96*, 587.

33. Steiner, L.A.; Eisen, H.N. *J. Exptl. Med.* **1967**, *126*, 1161.

34. McGuigen, J.E.; Simms, E.S.; Eisen, H.N. *Federation Proc.* **1966**, *25*, 677.

35. Lisowska-Bernstein, B.; Siskind, G.W.; Lamm, M.E. *Proc. Soc. Exptl. Biol. Med.* **1968**, *128*, 558.

36. Tramantano, A; Janda K.D.; Lerner, R.A. *Scinece* **1988**, *234*, 1570-1573.

37. Pollack, S.J.; Jacobs, J.W.; Schultz, P.G. *Science* **1986**, *234*, 1570-1573.

38. Schultz, P.G. *Angew. Chem. Int. Chem. Ed. Engl.* **1989**, *28*, 1283-1295.

39. Schultz, P. G. *Science* **1988**, *240*, 426-432.

40. Shokat, K.; Schultz, P.G. in "Methods in Enzymology Vol. 203," ed. by Langone, J.J., Academic Press, Inc., San Diego **1991**, 327-351.

41. Lerner, R.A.; Benkovic, S.J.; Schultz, P.G. *Science* **1991**, *252*, 659-667.

42. Napper, A.D.; Benkovic, S.J.; Tramantano, A.; Lerner, R.A. Science 1987, 1041-1043.

43. Hilvert, D.; Carpenter, S.H.; Nared, K.D.; Auditor, M.T. *Proc. Nat. Acad. Sci. USA* **1988**, *85*, 4953-4955.

44. Jackson, D.Y.; Jacobs, J.W.; Sugasawara, R.; Reich, S.H.; Bartlett, P.A.; Shultz, P.G. *J. Am. Chem. Soc.* **1988**, *110*, 4841-4842.

45. Hilvert, D.; Nared, K.D. *J. Am. Chem. Soc.* **1988**, *110*, 5593-5594.

46. Balan, A.; Coctor, B.P.; Green, B.; Torten, M.; Ziffer, H. *J. Chem. Soc. Chem. Comm.* **1988**, 106-108.

47. Cochran, A.G.; Schultz, P.G. *Science*, **1990**, *249*, 781-783.

48. Iverson, B.L.; Cameron, K.E.; Jahangiri, G.K.; Pasternak, D.S. *J. Am. Chem. Soc.* **1990**, *112*, 5320-5323.

49. Iverson, B.L.; Iverson, S.A.; Cameron, K.E.; Jahangiri, G.K.; Pasternak, D.S.; Lerner, R.A. in "Catalytic Antibodies, Ciba Foundation Symposium 159," John Wiley & Sons, New York 1991, 227-235.

50. Pollack, S.J.; Nakayama, G.R.; Schultz, P.G. *Science* **1988**, *242*, 1038-1040.

51. Iverson, B.L.; Lerner, R.A. *Science* **1989**, *243*, 1184-1188.

52. Pollack, S.J.; Schultz, P.G. *J. Am. Chem. Soc.* **1989**, *111*, 1929-1931.

53. Cochran, A.G.; Schultz, P.G. *J. Am. Chem. Soc.* **1990**, *112*, 9414-9415.

54. Nakayama, G.R.; Schultz, P.G. *J. Am. Chem. Soc.* **1992**, *114*, 770-782.

55. Lewis, C.; Kramer, T.; Robinson, S.; Hilvert, D. *Science* **1991**, *253*, 1019-1022.

56. Janda, K.D.; Ashley, J.A.; Jones, T.M.; Mcleod, D.A.; Schloeder, D.M.; Weinhouse, M.I. *J. Am. Chem. Soc.* **1990**, *112*, 8886-8888.

57. Ashley, J.A.; Janda, K.D. *J. Org. Chem.* **1992**, *57*, 6691-6693.

58. Hilvert, D.; Hill, K.W.; Nared, K.D.; Auditor, M. *J. Am. Chem. Soc.* **1989**, *111*, 9261-9262.

59. Braisted, A.C.; Schultz, P.G. *J. Am. Chem. Soc.* **1990**, *112*, 7430-7431.

60. Suckling, C.J.; Tedford, M.C.; Bence, L.M.; Irvine, J.I.; Stimson, W.H. *Bioorg. & Med. Chem. Lett.* **1992**, *2*, 49-52.

61. Benkovic, S.J.; Napper, A.D.; Lerner, R.A. *Proc. Nat. Acad. Sci. USA* **1988**, *85*, 5355-5358.

62. Janda, K.D.; Lerner, R.A.; Tramantano, A. *J. Am. Chem. Soc.* **1988**, *110*, 4835-4837.

63. Jacobsen, J.R.; Prudent, J.R.; Kochersperger, L.; Yonkovich, S.; Schultz, P.G. *Science* **1992**, *256*, 365-367.

64. Baldwin, E.; Schultz, P.G.; *Science*, **1989**, *245*, 1104-1107.

65. Tramantano, A.; Amman, A.A.; Lerner, R.A. *J. Am. Chem. Soc.* **1988**, *110*, 2282-2286.

66. Janda, K.D.; Benkovic, S.J.; Lerner, R.A. *Science* **1989**, *244*, 437-440.

67. Benkovic, S.J.; Adams, J.A.; Borders, C.L.; Janda, K.D.; Lerner, R.A. *Science* **1990**, *250*, 1135-1139.

68. Pollack, S.J.; Hsiun, P.; Schultz, P.G. *J. Am. Chem. Soc.* **1989**, *111*, 5691-5692.

89. Janda, K.D.; Schloeder, D.; Benkovic, S.J.; Lerner, R.A. *Science*, **1989**, *241*, 1188-1190.

70. Gibbs, R.A.; Taylor, S.; Benkovic, S.J. *Science* **1992**, *258*, 803-805.

71. Jacobs, J.; Sugasawara, R.; Powell, M.; Schultz, P.G. *J. Am. Chem. Soc.* **1987**, *109*, 2174-2176.

72. Wirsching, P.; Ashley, J.A.; Benkovic, S.J.; Janda, K.D.; Lerner, R.A. *Science* **1991**, *252*, 680-685.

73. Jackson, D.Y.; Schultz, P.G. *J. Am. Chem. Soc.* **1991**, *113*, 2319-2321.

74. Shokat, K.M.; Leumann, C.J.; Sugasawar, R.; Schultz, P.G. *Nature* **1989**, *338*, 269-271.

75. Scanlan, T.S.; Prudent, J.R.; Schultz, P.G. *J. Am. Chem. Soc.* **1991**, *113*, 9397-9398.

76. Cochran, A.G.; Sugasawara, R.; Schultz, P.G. *J. Am. Chem. Soc.* **1988**, *110*, 7888-7890.

77. Raso, V.; Stollar, D. *Biochmistry* **1975**, *14*, 584.

78. Schultz, P.G.; Jacobs, J.W. in "Environmental Influences and Recognition in Enzyme Chemistry," ed. by Liebman, H.R.; Greenberg, A., VCH Publishers, Inc., New York **1988**, 303-335.

79. Kohen, F.; Kim, J.B.; Barnard, G.; Lindner, H.R. *Biochem. st Biophys. Acta.* **1980**, *629*, 328.

80. Gallacher, G.; Jackson, C.S.; Topham, C.M.; Searcy, M.; Turner, B.C.; Badman, G.T.; Brocklehurst, K. *Biocem. J.* **1992**, *284*, 675.

81. Stephens, D.B.; Iverson, B.L. *Biochem. Biophys. Res. Comm.* **1993**, *192*, 1439-1444.

82. Wilmore, B.H.; Iverson, B.L. *J. Am. Chem. Soc.* **1994**, *116*, 2181-2182.

83. Stephens, D.B.; Wilmore, B.H.; Iverson, B.L. *Bioorg. and Med. Chem*, In Press.

84. Stephens, D.B.; Thomas, R.E.; Stanton, J.F.; Iverson, B.L. "A Study of Polyclonal Antibody Catalytic Variability," Submitted to Biochemistry.

85. Ingold, C.K. in "Structure and Mechanism in Organic Chemistry, $2^{nd}$ ed.," Cornell University Press, Ithaca **1953**, 1128-1191.

86. Richards, F.E.; Haber, E. *Federation Proc.* **1967**, *26*, 311.

87. Eisen, H.N.; Simms, E.S.; Little, J.R.; Styeiner, L.A. *Federation Proc.* **1964**, *23*, 559.

88. Parker, C.W.; Gott, S.M.; Johnson, M.C. *Biochemistry* **1966**, *5*, 2314.

89. Haber, E.; Richards, F.E.; Spragg, J.; Austen, K.F.; Vallotton, M.; Page, L.B. *Cold Spring Harbor Symp. Quant. Biol.* **1967**, *32*, 299.xx. Papenheimer, A.M.; Reed, W.P.; Brown, R. *J. Immunol.* **1968**, *100*, 1237.

90. Sela, M.; Mozes, E. *Proc. Nat. Acad. Sci.* **1966**, *55*, 445.

92. Amzel, L.M.; Poljak, R.J. *Ann. Rev. Biochem.* **1979**, *48*, 961-997.

93. Goodman, J.W. in "The Antigens," ed. by Sela, M., Academic Press, New York **975**, *3*, 127-187.

94. Iverson, B.L.; Shreder, K.; Kral, V.; Smith, D.; Sessler, J. *Pure Appl. Chem.* In Press.

95. Sessler, J.L.; Cyr, M.J.; Burrell, A.K. *Syn. Lett.* **1991**, *3*, 127-133.

96. Sessler, J.L.; Furuta, H.; Kral, V. *Supramolec. Chem.* **1993**, *1*, 209-220.

97. Furuta, H.; Cyr, M.J.; Sessler, J.L. *J. Am. Chem. Soc.* **1991**, *113*, 6677-6678.

98. Iverson, B.L.; Thomas, R.E.; Kral, V.; Sessler, J.L. *J. Am. Chem. Soc.* **1994**, *116*, 2663-2664.

99. Iverson, B.L.; Shreder, K.; Kral, V.; Sessler, J. *J. Am. Chem. Soc.* **1993**, *115*, 11022-11023.

100. Sessler, J.L.; Burrell, A.K. *Top. Curr. Chem.* **1991**, *161*, 177-273.

101. Woodward, R.B. in "Aromaticity: An International Symposium, Sheffield, Special Publication No. 21" The Chemical Society of London, **1966**.

102. Bauer, V.J.; Clive, D.L.J.; Dolphin, D.; Paine, J.B. III; Harris, F.l.; King, M.M.; Loder, J; Wang, S.W.C.; Woodward, R.B. *J. Am. Chem. Soc.* **1983**, *105*, 6429-6436.

103. Broadhurst, M.J.; Grig, R.; Johnson, A.W. *J. Chem. Soc. Perkin Trans. 1* **1972**, 2111-2116.

104. Sessler, J.L.; Cyr, M.J.; Lynch, V.; McGhee, E.; Ibers, J.A. *J. Am. Chem. Soc.* **1990**, *112*, 2810-2813.

105. Shinoya, M.; Furuta, H.; Lynch, V.; Harriman, A.; Sessler, J.L. *J. Am. Chem. Soc.* **1992**, *1142*, 5714-5722.

106. Sessler, J.L.; Cyr, M.J.; Furuta, H.; Kral, V.; Mody. T.; Morishima, T.; Shinoya, M.; Weghorn, S.; *Pure Appl. Chem.* **1993**, *65*, 393.

107. Furuta, H.; Cyr, M.J.; Sessler, J.L. *J. Am. Chem. Soc.* **1991**, *113*, 6677-6678.

108. Iverson, B.L.; Thomas, R.E.; Kral, V.; Sessler, J.L. *J. Am. Chem. Soc.* **1994**, *116*, 2663-2664.

109. Collman, J.P.; Chong, A.O.; Jameson, G.B.; Oakley, R.T.; Rose, E.; Schmittou, E.R.; Ibers, J.A. *J. Am. Chem. Soc.* **1981**, *103*, 516-533.

110. Banville, D.L.; Marzilli, L.G.; Wilson, W.D. *Biochem. Biophys. Res. Comm.* **1983**, *113*, 148-154

111. Fisher, L.M.; Kuroda, R.; Sakai, T.T. *Biochemistry* **1985**, 24, 3199-3207.

112. Sogah, G.D.Y.; Cram, D.J. *J. Am. Chem. Soc.* **1976**, *98*, 3038-3041.

113. Bradshaw, J.S.; Krakowiak, K.E.; Tarbet, B.J.; Bruening, R.L.; Biernat, J.; Bochenka, M.; Izatt, R.M.; Christensen, J.J. *Pure Appl. Chem.* **1989**, *61*, 1619-1624.

114. Izatt, R.M.; Bruening, R.L.; Tarbet, B.J.; Griffin, D.L.; Bruening, M.L.; Krakowiak, K.E.; Bradshaw, J.S.; *Pure Appl. Chem.* **1990**, *62*, 1115-1118.

115. Takagi, M.; Nakamura, H. *J. Coord. Chem.* **1986**, *15*, 53-82.

116. Kliza, D.M.; Meyerhoff, M.E. *Electroanalysis*, **1992**, *4*, 841-849.

117. Kibbey, C.E.; Meyerhoff, M.E. *Anal. Chem.* **1993**, *65*, 2188-2196.

118. Kokufuta, E.; Sodeyama, T.; Takeda, S. *Polymer Bull.* **1986**, *15*, 479-484.

119. Zon, G. in "HPLC in Biotechnology," ed. by Hancock, W.S., J. Wiley & Sons, New York **1990**, 301-398.

120. Chaiken, I.M.; Fassina, G,; Caliceti, P. in "High Performance Liquid Chromatography," J. Wiley & Sons, New York **1989**, 317-336.

121. Pederson, C.J. *J. Am. Chem. Soc.* **1967**, *89*, 7017.

122. Bradshaw, J.S.; Bruening, R.L.; Krakowiak, K.E.; Tarbet, B.J.; Izatt, R.M.; Christensen, J.J. *J. Chem. Soc. Comm.* **1988**, 812-814.

123. Schilde, U.; Uhlmann, E. *Reactive Polymers* **1993**, *20*, 181-188.

124. Brown, D.V.; Ckaniotakis, N.A.; Lee, I.H.; Ma, S.C.; Park, S.B.; Meyerhoff, M.E.; Nick, R.J.; Groves, J.T. *Electroanalysis* **1989**, *1*, 477-484.

125. Park, S.B.; Matuszewski, W; Meyerhoff, M.E.; Liu, Y.H.; Kadish, K.M. *Electranalysis* **1991**, *3*, 909-916.

126. Brown, P.R.; Roman, M.J. *J. Chrom.* **1992**, *592*, 3-12.

127. Bergot, B.J.; Egan, W. *J. Chrom.* **1992**, *599*, 35-42.

128. Tao, L.; Li, W. *J. Chrom.* **1992**, *607*, 19-24.

129. Smith, R.E.; MacQuarrie, R.A.; Jope, R.S. *J. Chrom. Sci.* **1991**, *29*, 528-531.

130. Polverelli, M.; Berger, M.; Odin, F.; Cadet, J. *J. Chrom.* **1993**, *613*, 257-265.

131. Cacia, J.; Quan, C.P.; Vasser, M.; Silkowski, M.B.; Frenz, J. *J. Chrom.* **1993**, *634*, 229-239.

132. Wilce, M.C.; Aguilar, M.I.; Hearn, M.T.W. *J. Chrom.* **1993**, *632*, 11-18.

133. Various authors in "Oligonucleotide Synthesis: A Practical Approach," ed. by Gait, M.J., IRL Press, Washington, D.C. **1984**, 1-217.

134. Various authors in "Chemical and Enzymatic Synthesis of Gene Fragments: A Laboratory Manual," ed. by Gasson, H.G.: Lang, A., Verlag Chemie, Weinham **1982**, 1-249.

135. Amari, J.V.; Brown, P.R.; Pivarnik, R.K.; Sehgal, R.K.; Turcotte, J.G. *J. Chrom.* **1992**, *590*, 153-161.

136. Takemoto, K.; Inaki, I.; Miyamoto, T.; Nagae, S. *Polymer. J.* **1989**, *21*, 19-33.

137. Rawn, J.D. "Biochemistry," Neil Patterson Publishers, Burlington, N.C. **1989**, 237-286.

138. Ng, M.; Blaschke, T.F.; Arias, A.A.; Zare, R.N. *Anal. Chem.* **1992**, *64*, 1682-1684.

139. Pearson, J.D.; Regnier, F.E. *J. Chrom.* **1983**, 255, 137-149.

140. Ramos, D.E.; Schoffstall, A.M. *J. Chrom.* **1983**, *261*, 83-93.

141. Engelhardt, H.; Beck, W.; Kohr, J.; Schmitt, T. *Angew. Chem.* **1993**, *32*, 629-766.

142. Sessler, J.L.; Hemmi, G.; Murai, T. *Inorg. Chem.* **1989**, *28*, 3390-3393.

143. Sessler, J.L.; Kral, V.; Furuta, H. *J. Am. Chem. Soc.* 1992, *114*, 8704-8705.

144. Fodor-Csorba, K. *J. Chrom.* **1992**, *624*, 353-367.

145. Snyder, J.L.; Grob, R.L.; McNally, M.E.; Oostdyk, T.S. *J. Chrom. Sci.* **1993**, *31*, 183-191.

146. Nishikawa, Y. *Anal. Sci.* **1992**, *8*, 681-686.

147. Grob, R.L. *J. Liq. Chrom.* **1993**, *16(8)*, 1783-1802.

148. Telliard, W.A. *J. Chrom. Sci.* **1990**, *28*, 453-459.

149. Loconto, P.R.; Gaind, A.K. *J. Chrom. Sci.* **1989**, *27*, 569-573.

150. Kostianin, R.; Bruins, A.P.; Hakkinen, V.M.A. *J. Chrom.* **1993**, *634*, 113-118.

151. Ember, L. *C & EN* **1993**, 8-9.

152. Ember, L. *C & EN* **1992**, 19-20.

153. Calender, D.W.; Ceceh, T.R. *Biochemistry* **1990**, *29*, 1355-1361.

154. Latham, J.A.; Cech, T.R. *Science* **1989**, *245*, 276-281.

155. Shannon, R.D. *Acta. Crystallogr.* **1976**, *A32*, 751-767.

156. Unger, K.K.; Becker, N.; Roumeliotis, P. *J. Chrom.* **1976**, *125*, 115-127.

157. Weber, S.G.; Carr, P.W. in "High Performance Liquid Chromatography," J. Wiley & Sons, New York **1989**, 1-116.

158. Skoog, D.A.; West, D.M. in "Fundamenatls in Analytical Chemistry, 3rd ed." Holt, Rinehart and Winston, New York **1976**.

## Vita

Richard Edward Thomas was born in Westwood, New Jersey on 11 June 1965, the son of Raymond Louis Thomas Sr. and Carol Blinn Thomas. After graduating from Roxbury High School, Succasunna, New Jersey, in 1983. He attended The Ohio State University in Columbus, Ohio on a Naval R.O.T.C. scholarship. He was commissioned an officer in the U.S. Navy, after receiving a Bachelor of Arts degree in chemistry in June, 1987. He attended and graduated from the Naval Nuclear Power School in Orlando, Florida. His next assignment involved extensive training and qualification officer at the S3G submarine nuclear reactor in Balston Spa, New York. Then he completed the Shipboard Division Officers Course in Newport, Rhode Island, graduating with distinction. Next he was assigned to the the nuclear powered aircraft carrier U.S.S. Abraham Lincoln (CVN-72), where he served as mechanical division officer and as the Reactor Training Officer. This tour of duty included participation in Operation Desert Storm. During this tour he qualified as Engineering Officer of the Watch, Officer of the Deck, Surface Warfare Officer, and Prospective Nuclear Engineering Officer. He entered the University of Texas at Austin in the fall of 1992. Currently he is an active duty Lieutenant in the United States Navy, pursuing a Master's degree. His next assignment will be to attend Department Head School in Newport, R.I., and subsequent assignment as a Department Head on a Naval Surface Combatant.

Permanent address: 905 Rigel
Friendswood, Texas 77546

This thesis was typed by the author.

DUDLEY KNOX LIBRARY
NAVAL POSTGRADUATE SCHOOL
MONTEREY CA 93943-5101

DUDLEY KNOX LIBRARY
3 2768 00019288 4